Reduced-order models for fluids, using balanced truncation and dynamically scaling modes

Clancy Rowley

1 April 2008
IMB – INRIA Bordeaux
Bordeaux, France

Mechanical
and Aerospace
Engineering
PRINCETON

Acknowledgements

- Acknowledgments
  - Students

    Milos Ilak
    (channel flow)

    

    Sunil Ahuja
    (airfoil separation)

    

  - Postdoc
    - Mingjun Wei (NMSU)
      (free shear flow)

    

  - Collaborators
    - Yannis Kevrekidis (Princeton)
    - Dave Williams (IIT)
    - Tim Colonius, Sam Taira (Caltech)
    - Gilead Tadmor (Northeastern)
  - Funding from NSF and AFOSR

Outline

- Approximate balanced truncation using POD
  - Importance of inner product for Galerkin projection
  - Balanced truncation
  - Method of snapshots
- Applications
  - Linearized channel flow
  - Separating flow past an airfoil
- Dynamically scaling POD modes
  - Free shear layer
  - Scaled basis functions
  - Template fitting
  - Equations for the shear layer thickness

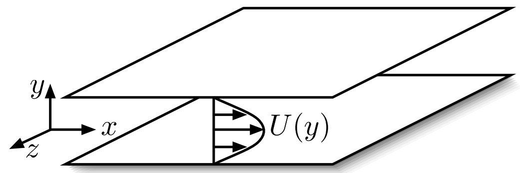

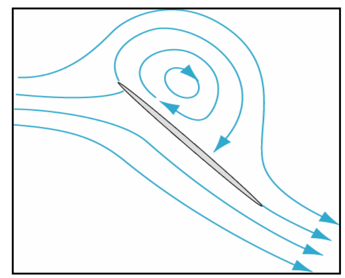

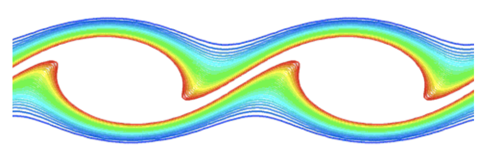

Galerkin projection

- Dynamics evolve on a high-dimensional space (or infinite-dim'l)
- Project dynamics onto a low-dimensional subspace S

$$\dot{x} = f(x) \qquad x \in V$$

$$r \in S \subset V$$

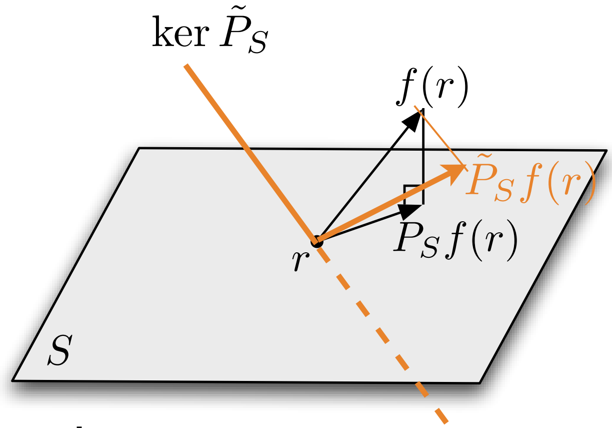

- Define dynamics on the subspace by

$$\dot{r} = P_S f(r) \qquad P_S : V \to S \text{ is a projection}$$

- Two choices:
  - choice of subspace
  - choice of inner product
    (equivalently, choice of the nullspace for a non-orthogonal projection)

Energy-based inner products

- Reduced-order models can behave unpredictably
  - Can even change stability type of equilibria
    [Rempfer, Thoret. CFD 2000]
  - Simple example: consider the system:

$$\frac{d}{dt}\begin{pmatrix} x_1 \\ x_2 \end{pmatrix} = \begin{pmatrix} 1 & -1 \\ 3 & -2 \end{pmatrix}\begin{pmatrix} x_1 \\ x_2 \end{pmatrix}$$

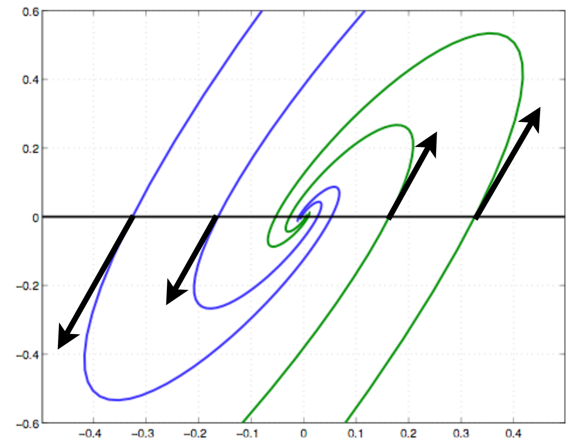

  - Sink at the origin
  - Projection onto x_1 axis is

$$\dot{x}_1 = x_1 \quad \text{unstable}$$

  - Can at least fix this simple problem by changing the inner product used for the projection
    - Cute result: If an orthogonal projection is used with an "energy-based" inner product, this will ensure stability of the origin
    - Note: does not guarantee stability preserved for other equilibrium points, periodic orbits, etc.

[Rowley, T Colonius, RM Murray, Phys D 2004]

Energy-based inner products

- Consider a system with a stable equilibrium point at the origin:

$$\dot{x} = f(x) \qquad f(0) = 0 \qquad x \in \mathbb{R}^n$$

- Consider an inner product whose induced norm is a Liapunov function ("energy-based"):

$$\langle x, y \rangle = x^T Q y, \qquad Q > 0 \qquad \begin{array}{l} V(x) = x^T Q x \text{ is a Liapunov function} \\ \dot{V}(x) = 2x^T f(x) \leq 0, \qquad \forall x \in U \end{array}$$

- Reduced-order dynamics given by orthogonal projection

$$\begin{array}{lll} r = Px & P^2 = P & \\ \dot{r} = Pf(r) & \langle x, Py \rangle = \langle Px, y \rangle & QP = P^T Q \end{array}$$

- Then V is a Liapunov function for the reduced-order system:

$$\begin{aligned} \dot{V}(r) &= 2r^T QPf(r) = 2r^T P^T Qf(r) = 2(Pr)^T Qf(r) \\ &= 2r^T Qf(r) \leq 0 \end{aligned}$$

- So: if an energy-based inner product is used, the origin is stable for the reduced-order system, regardless of the subspace used for the projection

Outline

- Approximate balanced truncation using POD
  - Importance of inner product for Galerkin projection
  - Balanced truncation
  - Method of snapshots
- Applications
  - Linearized channel flow
  - Separating flow past an airfoil
- Dynamically scaling POD modes
  - Free shear layer
  - Scaled basis functions
  - Template fitting
  - Equations for the shear layer thickness

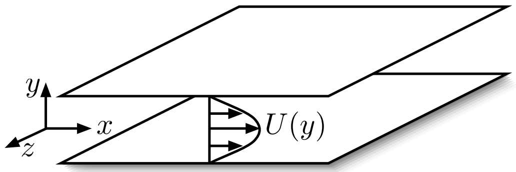

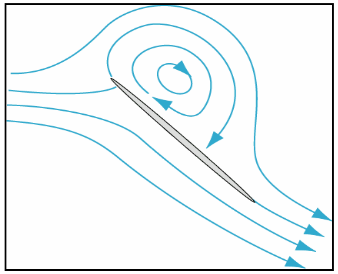

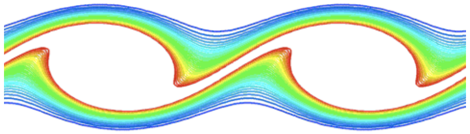

Are POD modes optimal?

- POD modes are not optimal for Galerkin projection
  - POD determines a subspace that optimally captures the energy in a given dataset
  - These modes are usually not optimal for Galerkin projection
    - Low-energy modes can play an important role in the dynamics [Aubry, Holmes, Lumley, 1988; Smith 2002 PhD thesis, Princeton]
  - Can often do better with balanced truncation [Moore 1981]

Error: ∞-norm

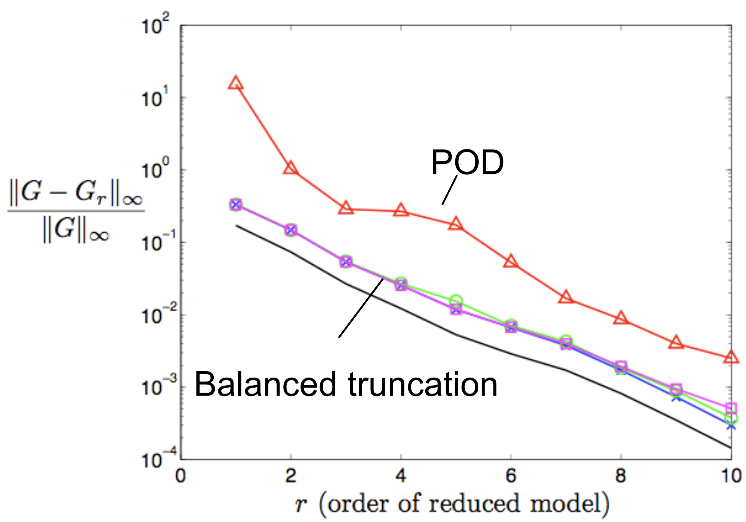

Balanced truncation

- Why doesn't everybody use this?
  - Valid for stable, linear systems
    - Extensions for unstable systems [Jonckheere & Silverman 1983, Zhou 2001]
    - Extensions for nonlinear systems [Scherpen 1993, Lall, Marsden, Glavaski 1999]
  - Computationally expensive for large systems
    - n^3 computational time: $n > 10^5$ for typical fluids simulations
- Improvements for large systems
  - POD is tractable for large systems. Can we extend, e.g., the method of snapshots, to compute balancing transformations?
  - Based on earlier snapshot-based methods:

    Lall, Marsden, & Glavaski, 1999
    Willcox & Peraire, 2001

Overview of balanced truncation

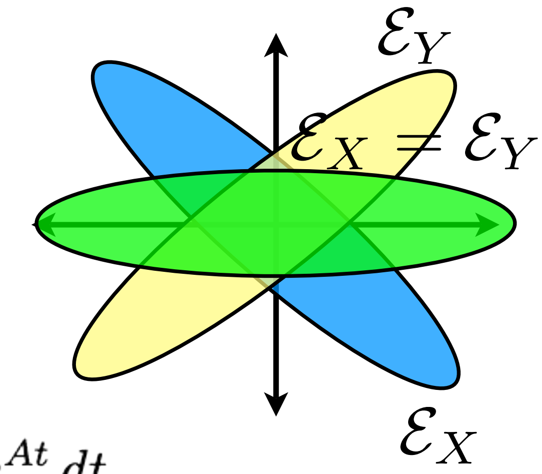

- Start with a stable, linear input-output system

$$\dot{x} = Ax + Bu$$
$$y = Cx$$

What are you interested in capturing?

- Compute controllability and observability Gramians

$$X = \int_0^\infty e^{At} BB^* e^{A^*t}\, dt \qquad Y = \int_0^\infty e^{A^*t} C^* C e^{At}\, dt$$
$$AX + XA^* + BB^* = 0 \qquad A^*Y + YA + C^*C = 0$$

States easily excited by an input

States that have large influence on the output

- Find a transformation T that simultaneously diagonalizes X and Y

$$x = Tz, \qquad T^{-1}X(T^{-1})^* = T^*YT = \Sigma = \begin{bmatrix} \sigma_1 & & \\ & \ddots & \\ & & \sigma_n \end{bmatrix}$$

- Change coordinates, and truncate states that are least controllable/observable

Empirical Gramians

- Construct Gramians from impulse response data
  - Not solving Liapunov equations
  - For a single input: compute impulse-state response:

solution
$$\dot{x} = Ax, \qquad x(0) = B$$
$$x(t) = e^{At}B$$

  - The controllability Gramian is then $$W_c = \int_0^\infty x(t)x(t)^T\,dt$$
  - Discretize in time, collect snapshots into a matrix:
$$X = \begin{bmatrix} | & & | \\ x(t_1) & \cdots & x(t_m) \\ | & & | \end{bmatrix}$$
  - Then $\boxed{W_c \approx XX^T}$
  - For observability Gramian, same procedure, but use adjoint equations $\dot{z} = A^* z \qquad z(0) = C^*$
  - For multiple inputs/outputs, same procedure, but do one impulse-response for each input/output

[Lall et al, 1999]

Method of snapshots

- POD: method of snapshots vs. direct method

$$X = \begin{bmatrix} | & & | \\ x_1 & \cdots & x_m \\ | & & | \end{bmatrix}$$

POD modes (direct method):

$$XX^T\varphi = \lambda\varphi \qquad n \times n$$

POD modes (method of snapshots):

[Sirovich, Q Appl Math 1987]

$$\varphi = Xc$$

$$X^TXc = \lambda c \qquad m \times m$$

  - method of snapshots more efficient when $m < n$.

- Balanced truncation: method of snapshots
  - Empirical Gramians represented as $W_c = XX^T$ $\quad n \times n$
    $W_o = YY^T$
  - Find a balancing transformation with an SVD of Y^TX $\quad m_y \times m_x$

[Rowley, Int. J Bif Chaos, 2005]

Computing modes

- Snapshot matrices

$$X = \begin{bmatrix} | & & | \\ x(t_1) & \cdots & x(t_m) \\ | & & | \end{bmatrix} \qquad Y = \begin{bmatrix} | & & | \\ z(t_1) & \cdots & z(t_l) \\ | & & | \end{bmatrix}$$

Linearized snapshots   Adjoint snapshots

- Compute SVD

$$Y^* X = U \Sigma V^*$$

- Obtain bi-orthogonal set of modes:

$$\Phi_r = \begin{bmatrix} | & & | \\ \varphi_1 & \cdots & \varphi_r \\ | & & | \end{bmatrix} \qquad \Psi_r = \begin{bmatrix} | & & | \\ \psi_1 & \cdots & \psi_r \\ | & & | \end{bmatrix}$$

Direct modes
linear combinations of
direct snapshots

Adjoint modes
linear combinations of
adjoint snapshots

$$\Phi = X V_r \Sigma_r^{-1/2} \qquad \Psi = Y U_r \Sigma_r^{-1/2}$$

$$\Psi_r^* \Phi_r = I_r$$

Reduced-order models

- Original equations

$$\dot{x} = Ax + Bu$$
$$y = Cx + Du$$

- Form reduced-order model
  - Do not need to transform entire state: just take first r modes

$$\dot{a} = \Psi_r^* A \Phi_r a + \Psi_r^* B u$$
$$y = C\Phi_r a + Du$$

- Extensions to nonlinear systems straightforward
  - For instance, compute modes for linearized system, project nonlinear dynamics

$$\dot{x} = f(x) \longrightarrow \begin{aligned} x(t) &= \sum_{j=1}^{r} a_j(t)\varphi_j \\ \dot{a}_j(t) &= \langle \psi_j, f(x) \rangle \end{aligned}$$

Large numbers of outputs

- Often, we are interested in modeling the full state
  - If dimension is large, project output onto POD modes
  - POD gives optimally-close output-projected system (in 2-norm)

u

$$\dot{x} = Ax + Bu$$
$$y = x$$

Full state

Original system, full dynamics

Output projection

u

$$\dot{x} = Ax + Bu$$
$$y = Cx$$

POD coefficients

Output-projected system, full dynamics

Balanced truncation

u

$$\dot{a} = \Psi^T A \Phi a + \Psi^T B u$$
$$y = C \Phi a$$

POD coefficients

Reduced-order model

Approximate balanced truncation for large systems

- Method of snapshots enables one to compute approximate balanced truncations with cost similar to POD
  - One simulation for each control input, one adjoint simulation for each output
  - One SVD, (# direct snapshots) x (# adjoint snapshots)
  - If number of outputs is large, method for projection onto smaller-rank output
- Balanced truncation is just POD with respect to an inner product defined by the observability Gramian Y:

$$\langle x_1, x_2 \rangle_Y = x_1^T Y x_2$$

- Observability Gramian is always a Liapunov function => preserves stability!
- Obtain set of bi-orthogonal modes:

direct modes: $\{\varphi_1, \ldots, \varphi_n\}$

adjoint modes: $\{\psi_1, \ldots, \psi_n\}$

bi-orthogonal: $\langle \psi_i, \varphi_j \rangle = \delta_{ij}$

Galerkin:

$$\dot{x} = f(x)$$

$$x(t) = \sum_j a_j(t) \varphi_j$$

$$\dot{a}_j(t) = \langle \psi_j, f(x) \rangle$$

Outline

- Approximate balanced truncation using POD
  - Importance of inner product for Galerkin projection
  - Balanced truncation
  - Method of snapshots
- **Applications**
  - **Linearized channel flow**
  - Separating flow past an airfoil
- Dynamically scaling POD modes
  - Free shear layer
  - Scaled basis functions
  - Template fitting
  - Equations for the shear layer thickness

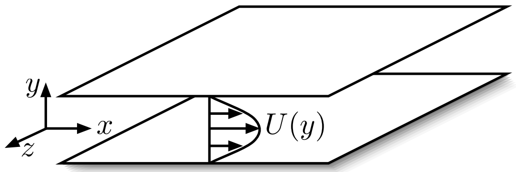

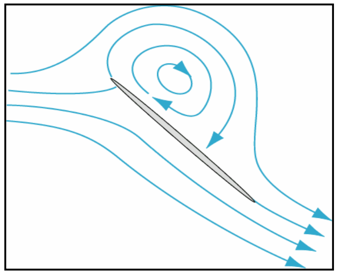

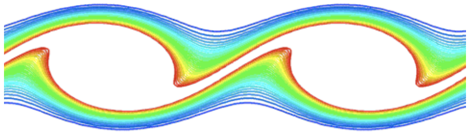

Application: Linearized Channel Flow

- Plane channel flow with periodic boundary conditions
  - Goal: delay transition to turbulence using feedback control
  - Goal: improved understanding of transition mechanisms
  - Focus: low-dimensional models of transition

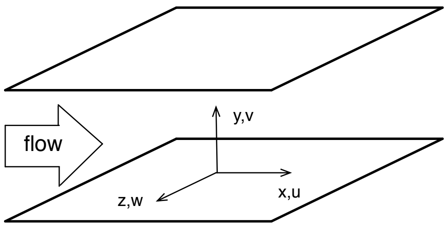

- Linear development of small perturbations
  - Transition not predicted correctly by linear stability analysis
  - Non-normality of the governing operator results in large transient growth of exponentially stable perturbations
  - Large linear system with complex dynamic behavior

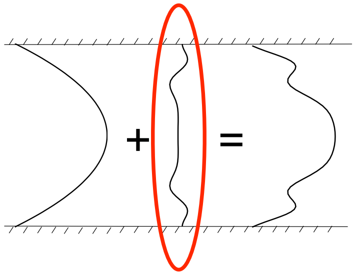

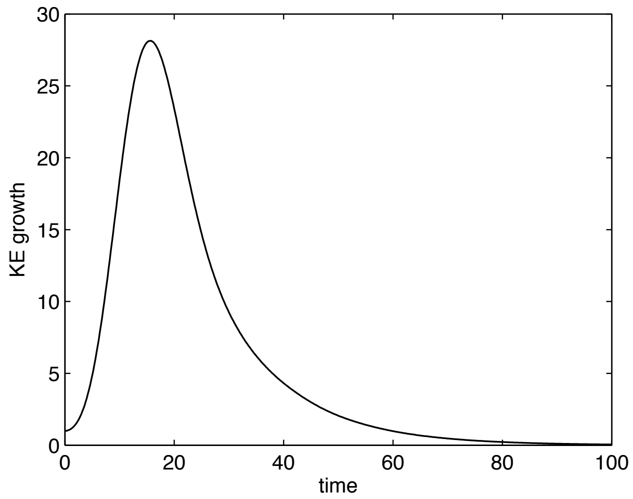

Previous work:
Trefethen et al [Science, 1993]
Farrell & Ioannou [96,96,01]
Schmid & Henningson [01]
Bamieh & Jovanovic [01,03]

Governing Equations

- Navier-Stokes equations linearized about a laminar profile
- Perturbation dynamics fully described by wall-normal velocity v and wall-normal vorticity η
- Clamped boundary conditions $v(\pm 1) = \frac{\partial v}{\partial y}(\pm 1) = 0$

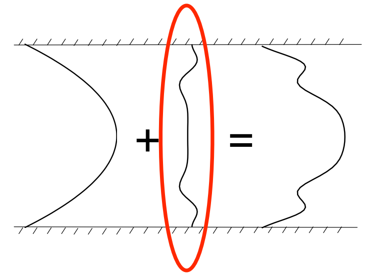

Orr-Sommerfeld/Squire system

$$\frac{\partial}{\partial t}\begin{bmatrix}-\Delta & 0 \\ 0 & I\end{bmatrix}\begin{bmatrix}v \\ \eta\end{bmatrix} = \begin{bmatrix}L_{OS} & 0 \\ -U'\partial_z & L_{SQ}\end{bmatrix}\begin{bmatrix}v \\ \eta\end{bmatrix}$$

$$L_{OS} = U\partial_x\Delta - U''\partial_x - \frac{1}{Re}\Delta^2$$

$$L_{SQ} = -U\partial_x + \frac{1}{Re}\Delta$$

Adjoint system

$$\frac{\partial}{\partial t}\begin{bmatrix}-\Delta & 0 \\ 0 & I\end{bmatrix}\begin{bmatrix}v \\ \eta\end{bmatrix} = \begin{bmatrix}L^*_{OS} & U'\partial_z \\ 0 & L^*_{SQ}\end{bmatrix}\begin{bmatrix}v \\ \eta\end{bmatrix}$$

$$L^*_{OS} = -U\partial_x\Delta - 2U'\partial_x\partial_y - \frac{1}{Re}\Delta^2$$

$$L^*_{SQ} = U\partial_x + \frac{1}{Re}\Delta$$

actuation

disturbances

$$\dot{x} = Ax + \underbrace{B}_{\text{actuation}}u_1 + \underbrace{F}_{\text{disturbances}}u_2$$

- System in standard state-space form with actuation and disturbances

Single-wavenumber perturbation - optimal

- Perturbations of the form

$$q = \hat{q}(y)e^{i\alpha x + i\beta z + \lambda t} \qquad q = \begin{bmatrix} v \\ \eta \end{bmatrix}$$

- System can be analyzed in 1-D so that full balanced truncation is tractable, allowing comparison with the BPOD approximation and POD
- Well-studied cases (Farrell, Henningson, Reddy, Schmid, Jovanovic, Bamieh)
- Case presented here α=1, β=1 and exhibits rich dynamics

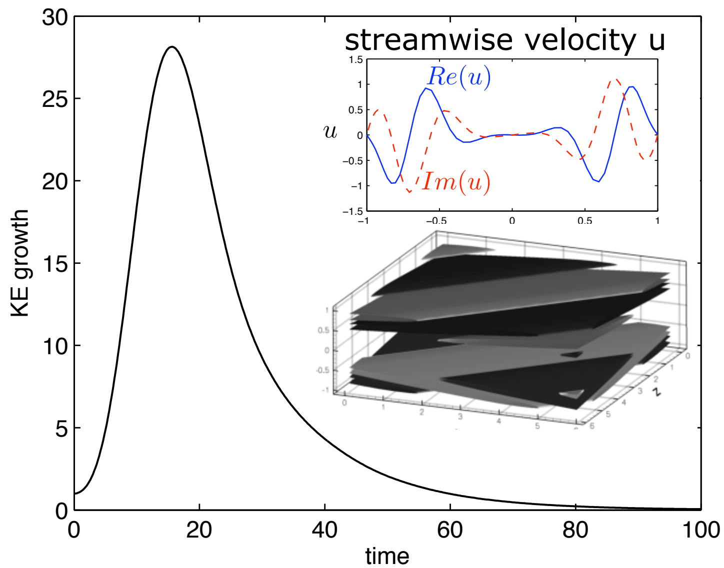

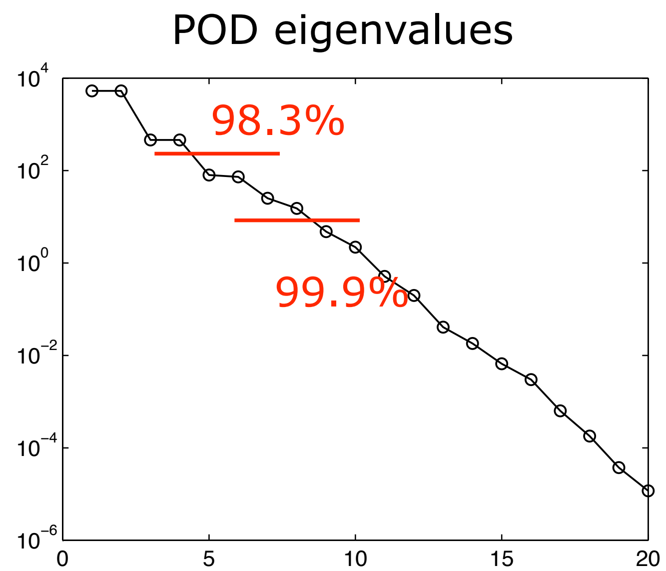

Modes and HSV - how good is BPOD?

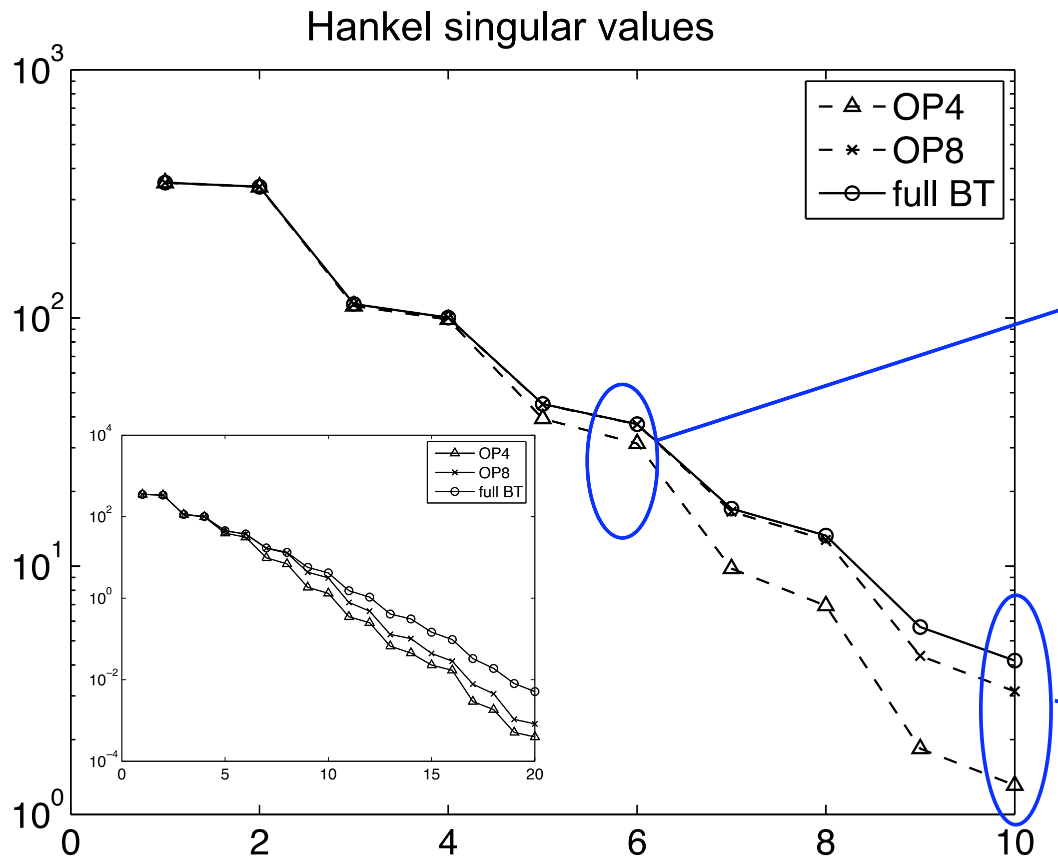

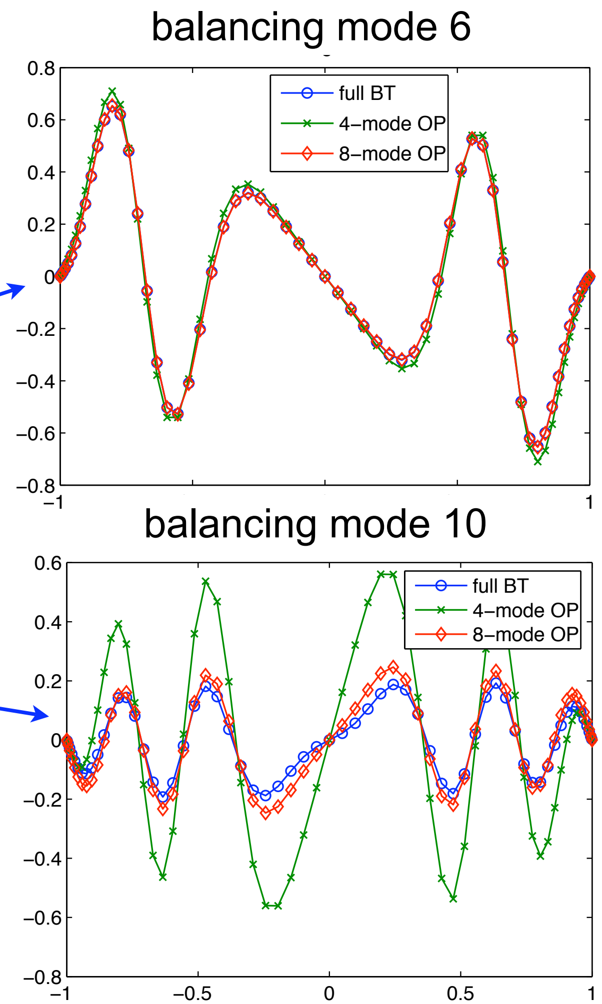

Both HSVs and balancing modes computed accurately up to approximately the rank of OP

Single wavenumber - impulse response

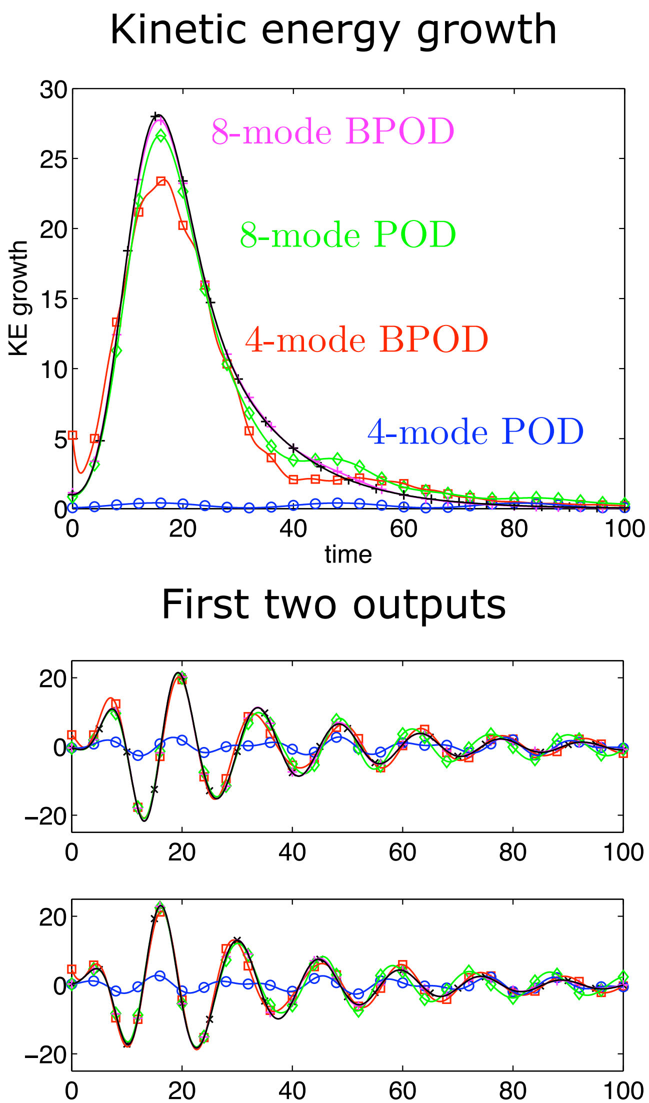

- Low-order POD models completely fail to capture energy growth
- BPOD model performance matches exact BT approximately up to the desired level of accuracy, determined by the output projection

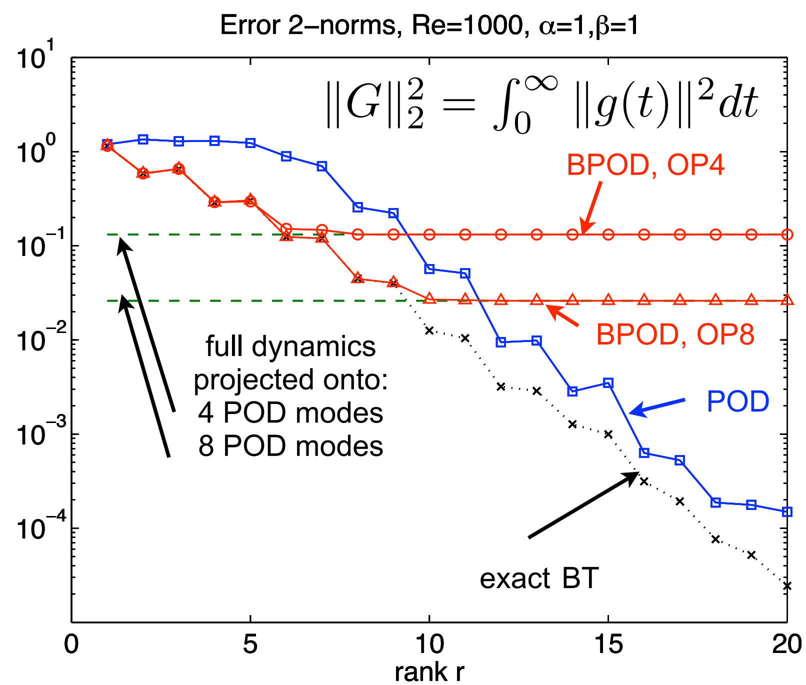

Single wavenumber - frequency response

- For a single wavenumber, frequency response can be computed exactly
- BPOD captures the resonant peak even at low order
- POD slowly catches up, but has spurious peaks due to eigenvalues near the imaginary axis

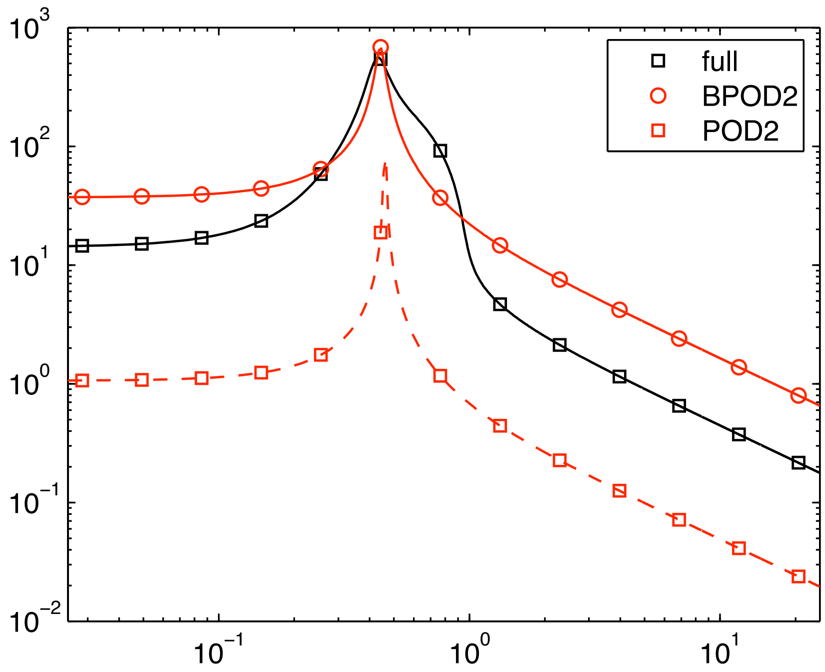

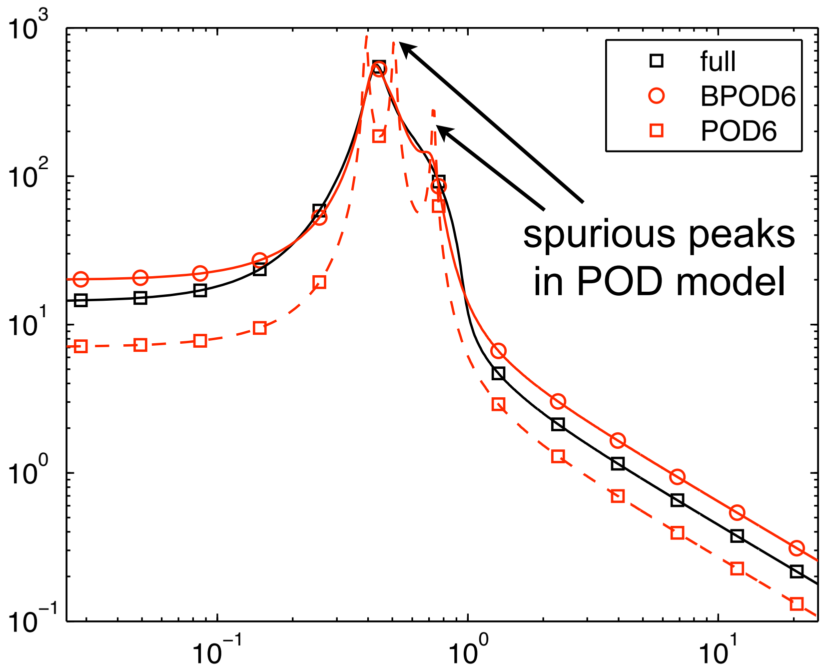

Single wavenumber - infinity norms

Infinity error norm bounds $\sigma_{r+1} \leq \|G - G_r\|_\infty \leq 2\Sigma_{j=r+1}^{n}\sigma_j$

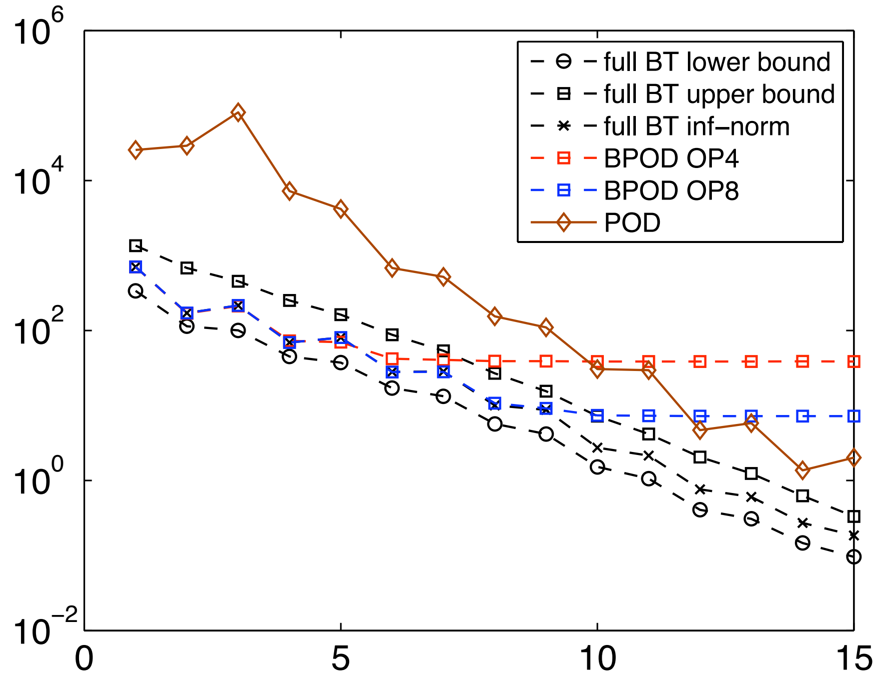

- Infinity norms of models also match those of exact BT up to approximately the rank of the output projection
- Again, POD 'catches up' only at a high rank

Localized actuator

- Periodic array of localized actuators in center of channel
- Large system (32x65x32), 133,120 states, exact BT intractable
- Impulse response snapshots obtained via linearized DNS, Re=2000
- Complex initial transient which develops into a streamwise-constant structure

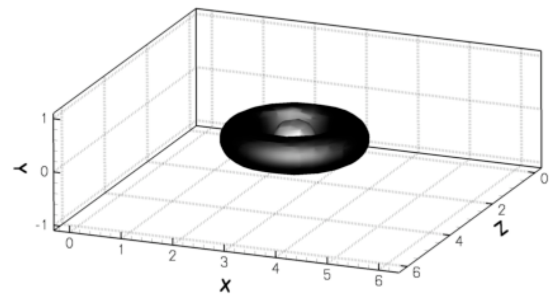

initial condition

POD eigenvalues

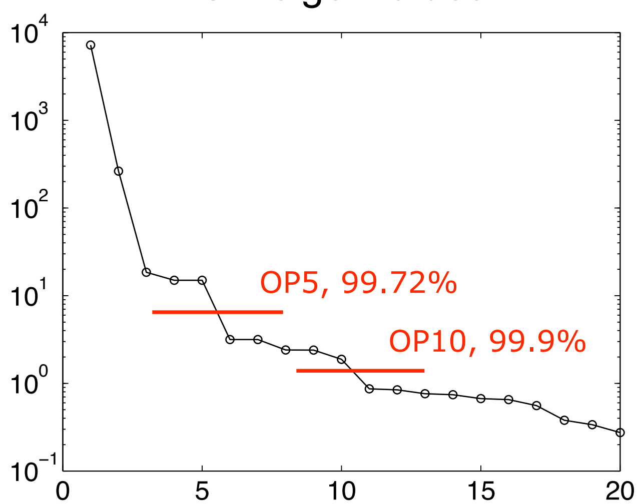

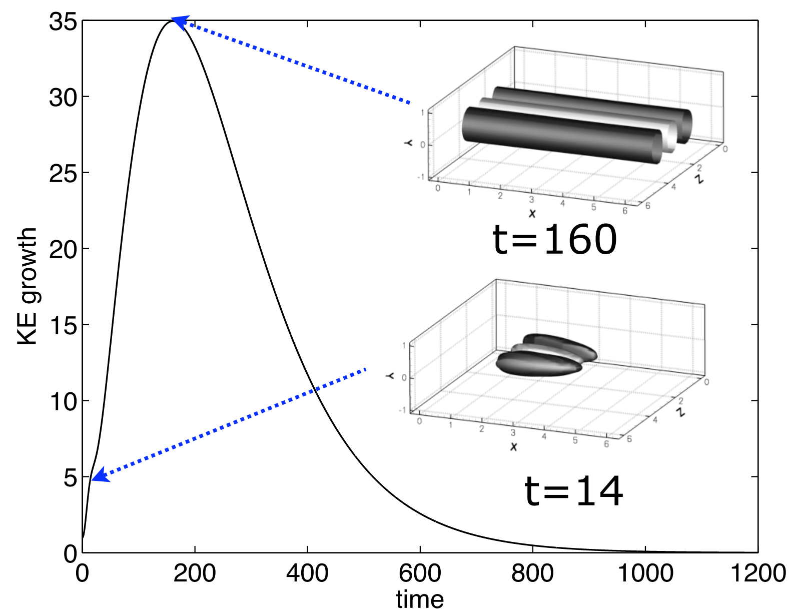

Localized actuator - POD model performance

POD modes 1-3

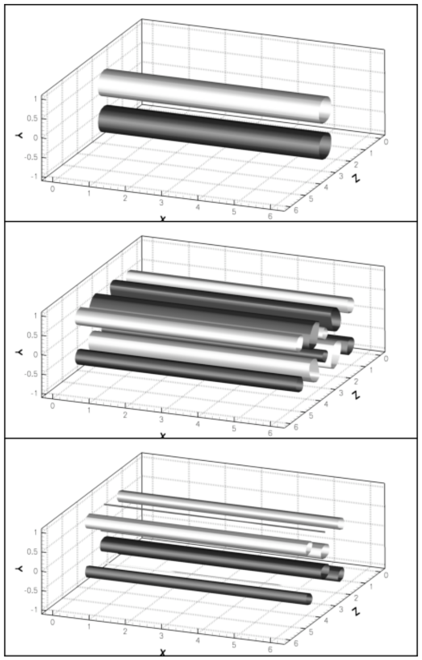

Standard POD

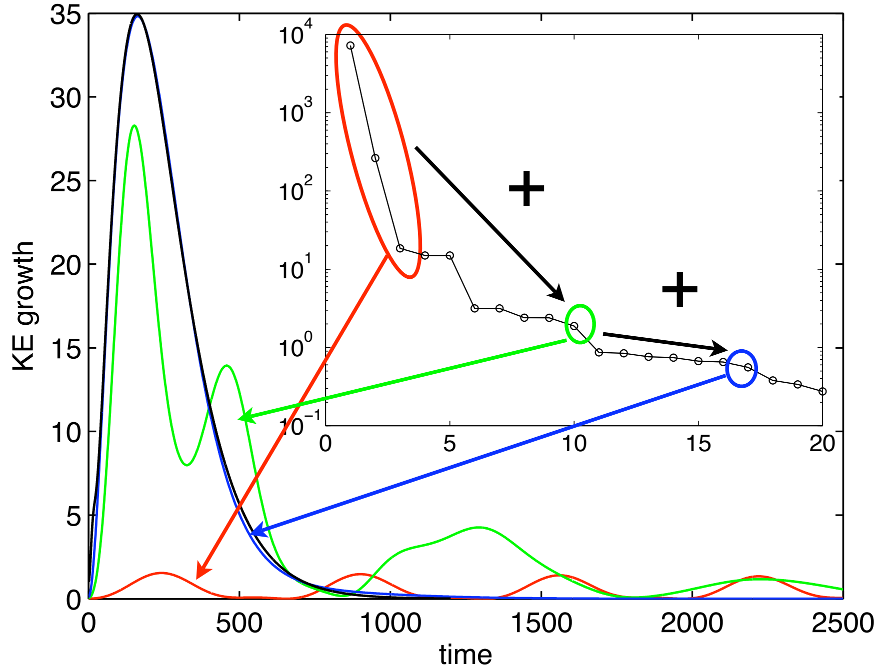

POD modes 4-5

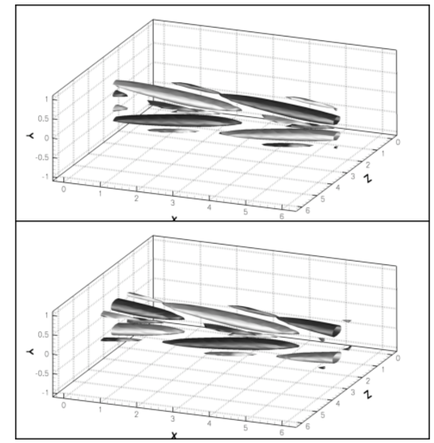

POD mode 10

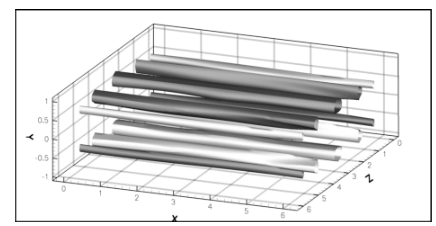

POD mode 17

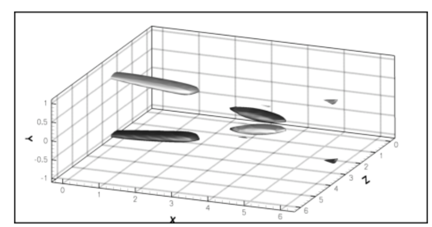

- Some low-energy POD modes are very important for the system dynamics - can't naively use just the most energetic ones
- Pairs of modes corresponding to traveling structures not important for capturing energy growth
- For many POD low-order models, the output can have spurious oscillations due to the mode pairs

Localized actuator - BPOD impulse response

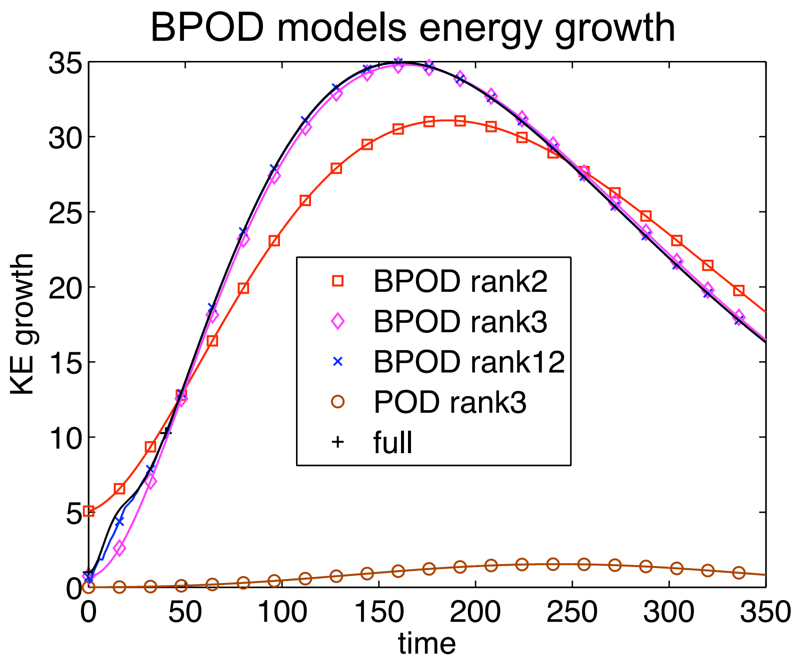

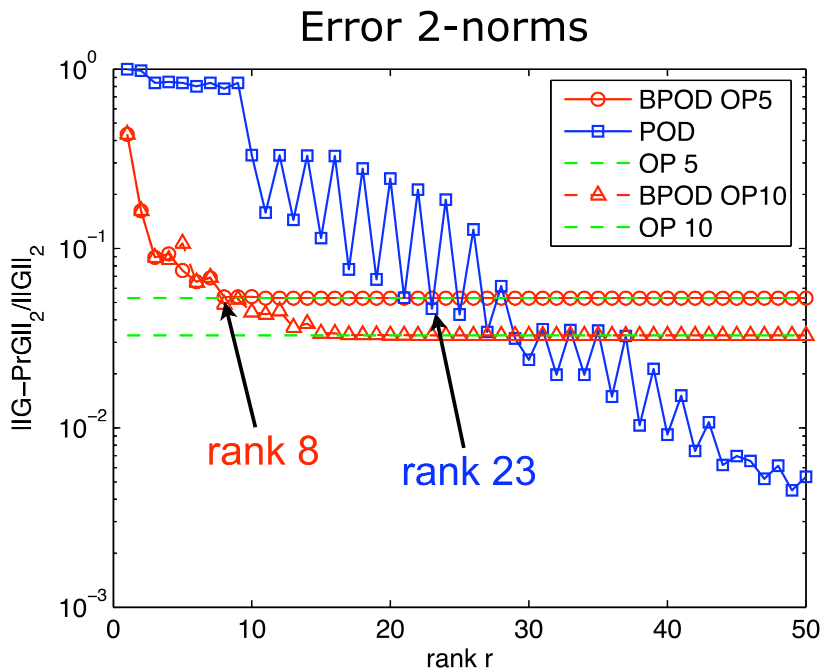

- Three-mode BPOD model excellent at capturing the energy growth
- Rank 8 BPOD model sufficient to correctly capture the dynamics of the first five POD modes, compared to at least 23 POD modes
- Inclusion of some POD modes significantly deteriorates performance (splitting of the pairs of oscillating modes)

Localized actuator - modes

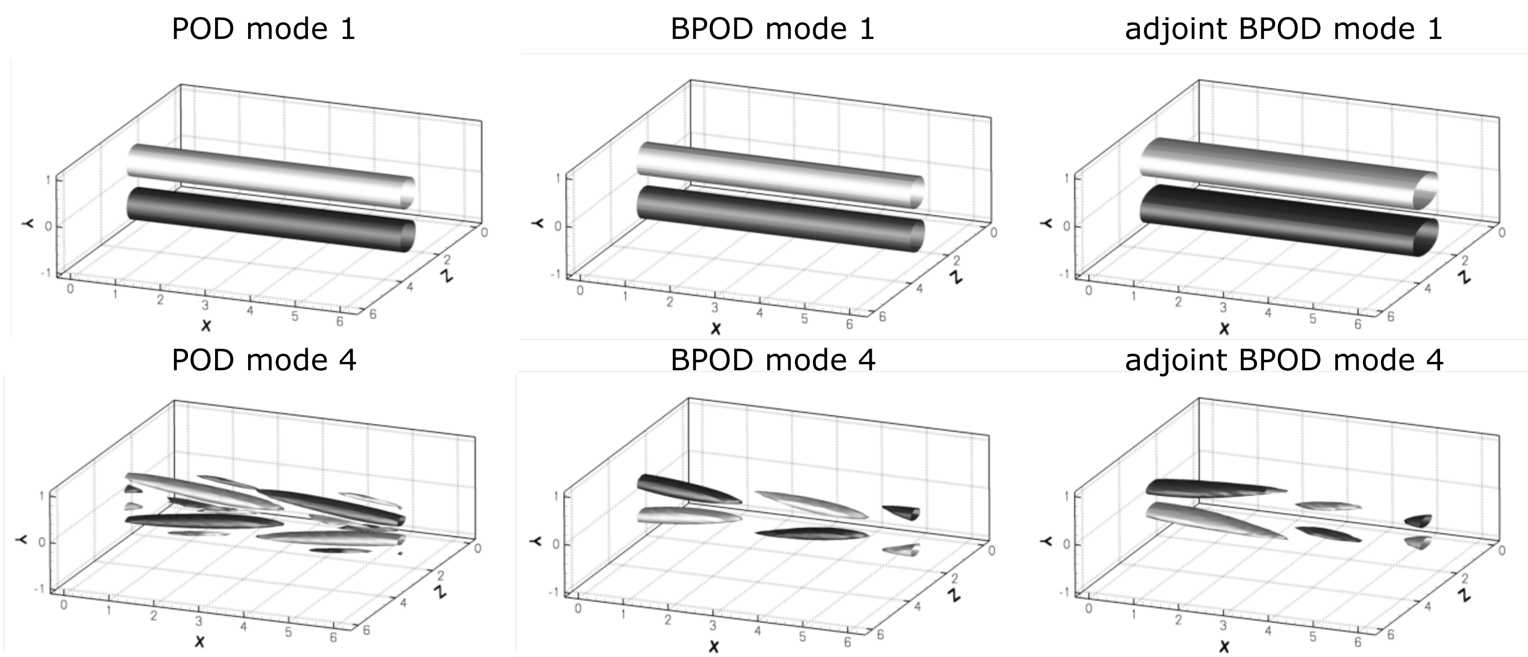

BPOD and adjoint BPOD modes from OP5

Balancing modes and POD modes look similar but the adjoint modes are in general quite different => different dynamics of models

POD

$$\dot{a}_j(t) = \langle \underline{\phi_j}, f(x) \rangle$$

BPOD

$$\dot{a}_j(t) = \langle \underline{\psi_j}, f(x) \rangle$$

Localized actuator - frequency response

POD singular value Bode plot

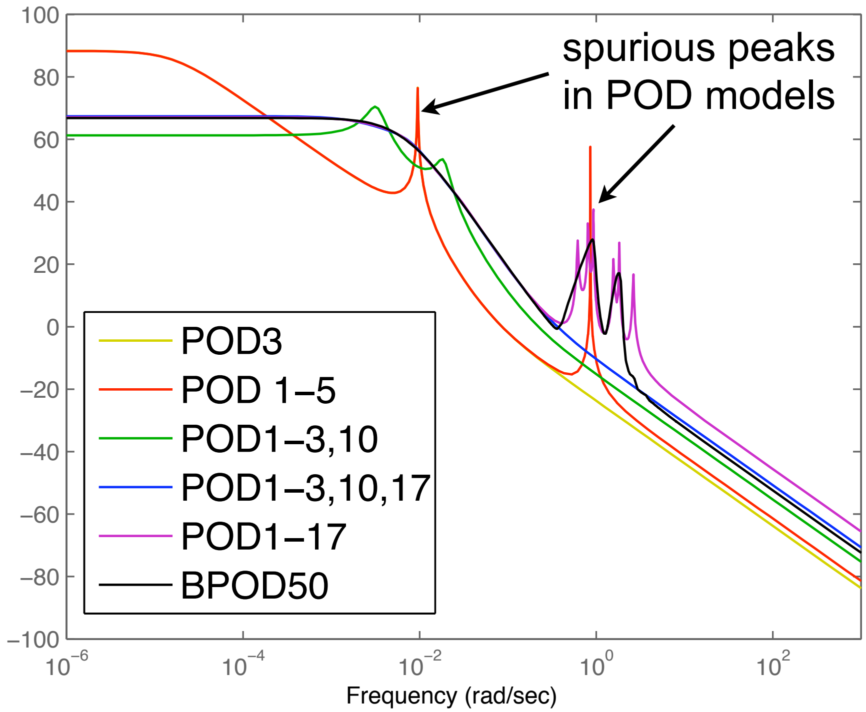

BPOD singular value Bode plot

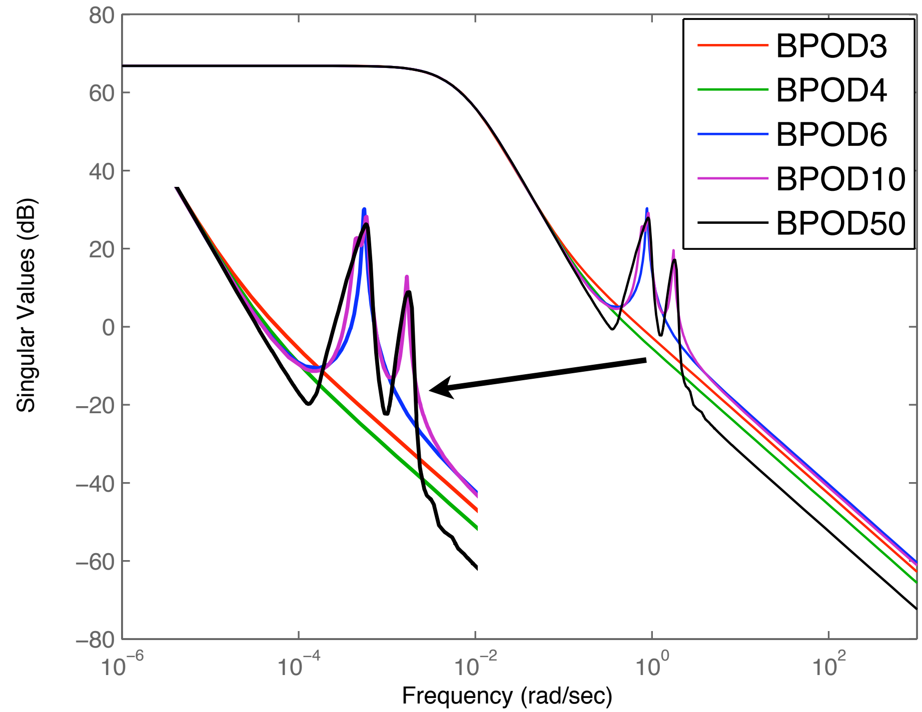

- BPOD 10-mode OP 50-mode model taken as ‘full system’
- POD poorly captures low-pass behavior, spurious peaks
- Need pairs of BPOD modes to capture peaks

Closed-loop control - localized actuator

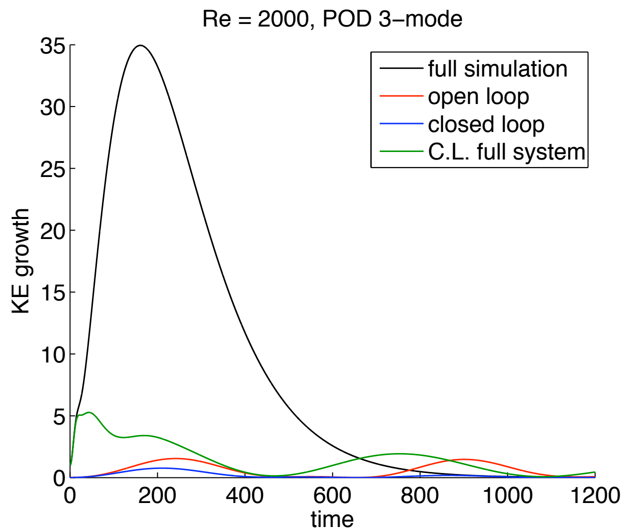

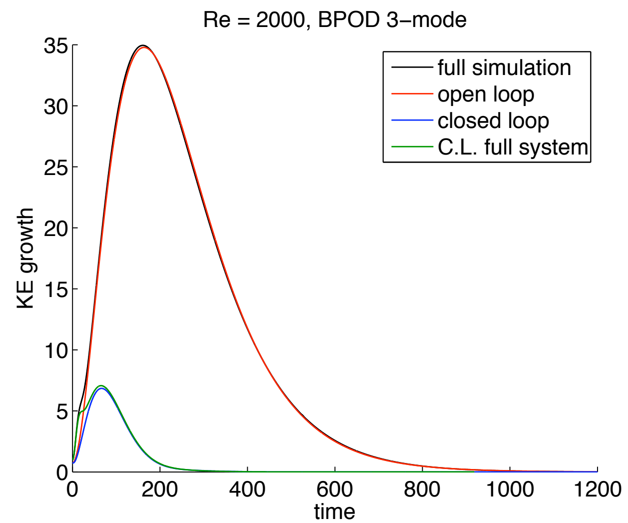

- Using the localized actuator to control a disturbance in channel center
- Standard LQR controller
- Using control gains from a 3-mode BPOD model reduces energy growth by a factor of 5
- BPOD works well in closed-loop at off-design condition (Re=5000 with modes from Re=2000)

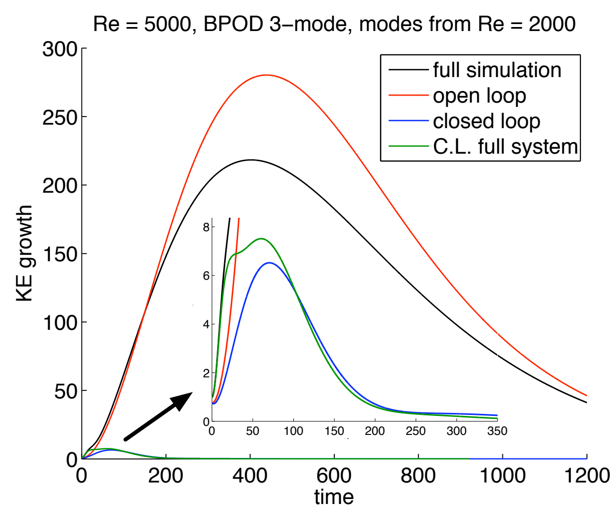

Nonlinear Evolution of the Localized Perturbation

linear evolution of wall-normal velocity

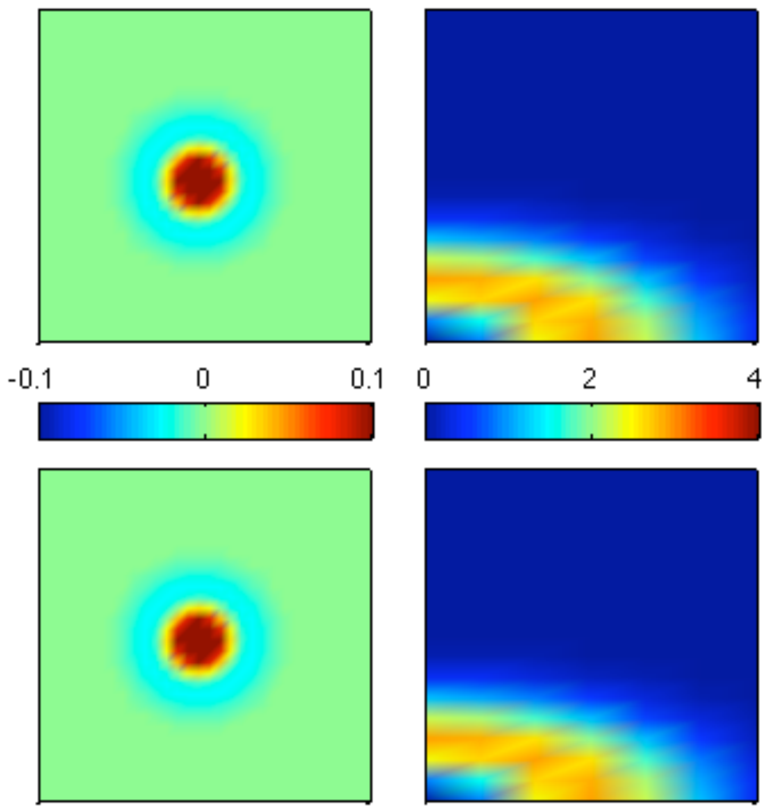

nonlinear evolution at $E_0/E_{lam} = 3.323 \times 10^{-4}$

- The spatial Fourier transform of the x,z plane at y=0 illustrates the perturbation evolution
- In the linear case the wavenumbers decay independently after the large transient growth
- $E_{lam} = 0.2667$ is the energy density of the mean laminar flow
- Transition for very small values of initial energy E_0
- The so-called β-cascade [Henningson et al, 1993] is observed in the nonlinear evolution - higher spanwise wavenumbers are introduced rapidly

Delaying Transition Using Feedback Control

- Try to increase the transition threshold of a localized perturbation (after Reddy et al)
- The threshold is defined as the energy density of the initial perturbation above which the flow transitions to turbulence
- Threshold found to be at $E_0 = 1.614 \times 10^{-4}$ of the mean flow energy of the laminar profile, $E_{lam} = 0.2667$

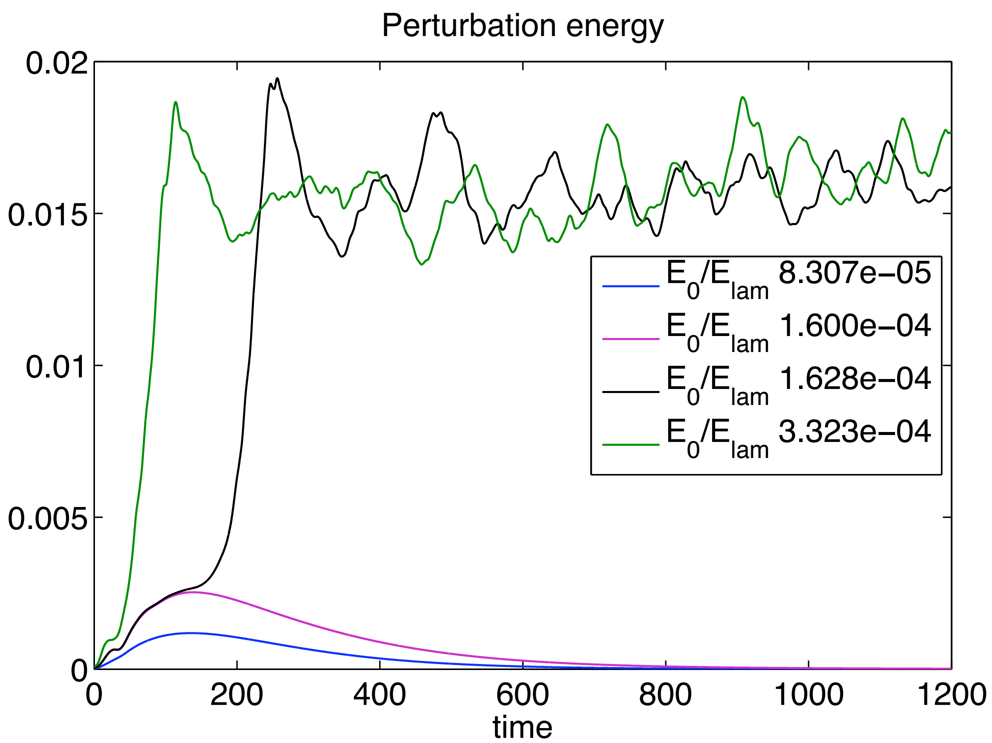

Closed-Loop Control

- The feedback gains computed using LQR for the linear system are used in a full nonlinear simulation with $E_0/E_{lam} = 3.323 \times 10^{-4}$
- An ‘aggressive’ controller (R=0.1 in LQR) manages to suppress the disturbance

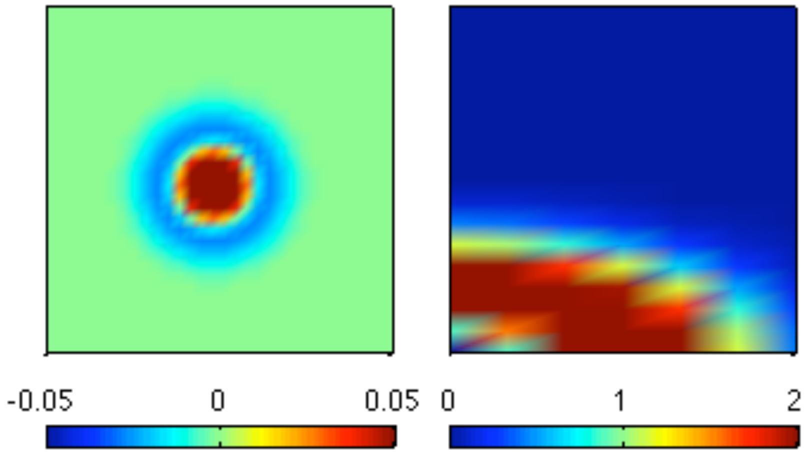

- Explanation: the BPOD modes do not have components at high β, and are not able to suppress high betas once they arise, but the ‘aggressive’ controller suppresses low β wavenumbers so that the higher β’s emerge at very low amplitudes and decay linearly
- Transition threshold increased by a factor of 17 for R=0.01
- Work in progress: see how projection of full N-S equations onto linear BPOD modes will model the perturbation evolution, and possibly design a nonlinear controller

Outline

- Approximate balanced truncation using POD
    - Importance of inner product for Galerkin projection
    - Balanced truncation
    - Method of snapshots
- Applications
    - Linearized channel flow
    - Separating flow past an airfoil
- Dynamically scaling POD modes
    - Free shear layer
    - Scaled basis functions
    - Template fitting
    - Equations for the shear layer thickness

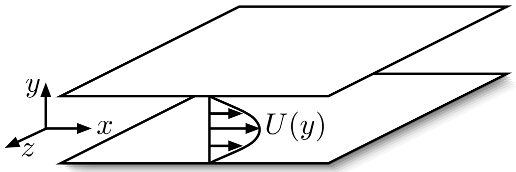

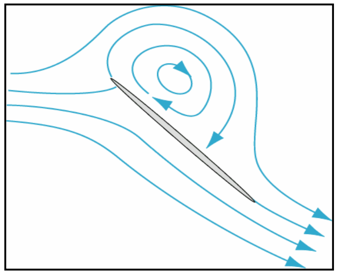

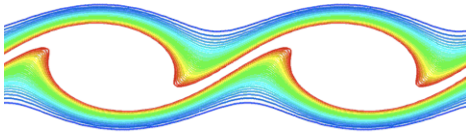

Motivation

- Leading edge vortices sometime provide high lift
- MURI goal: Stabilize these LEVs using feedback control
- High transient lift in pitching airfoils due to dynamic stall vortex

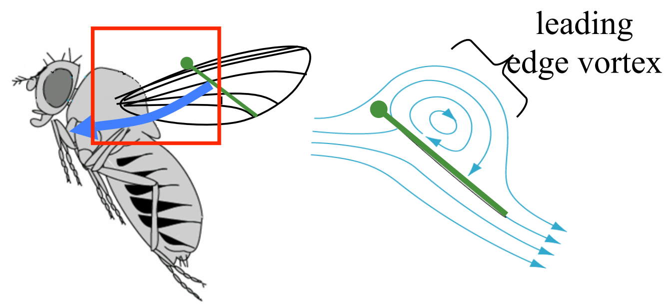

Pitching airfoil

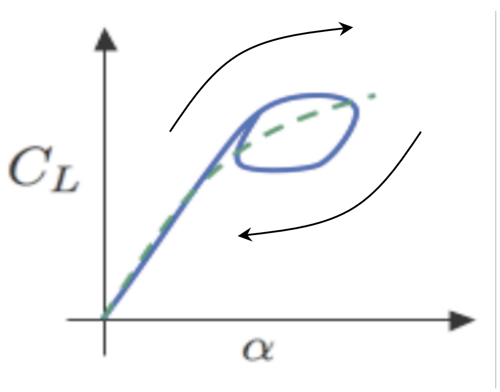

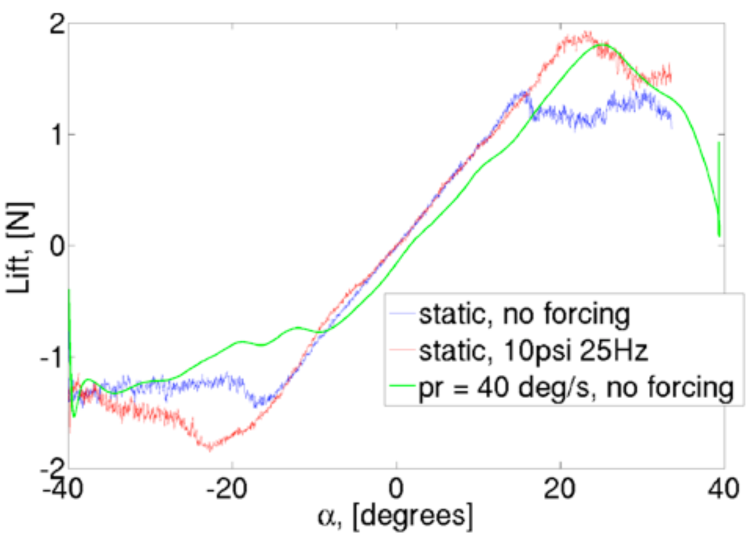

Dynamical behavior

- With increasing AoA, flow undergoes a Hopf bifurcation
- Reduced order models to stabilize unstable steady states at high AoAs

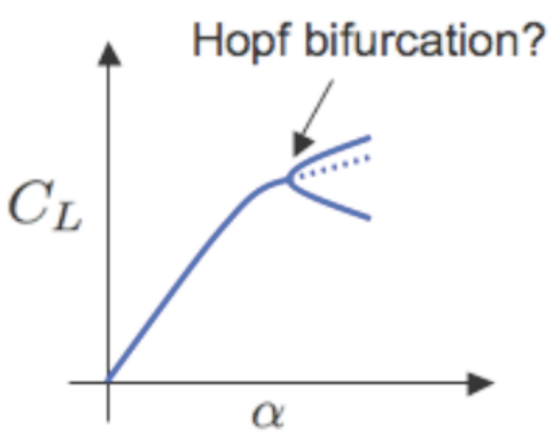

C_L at steady state

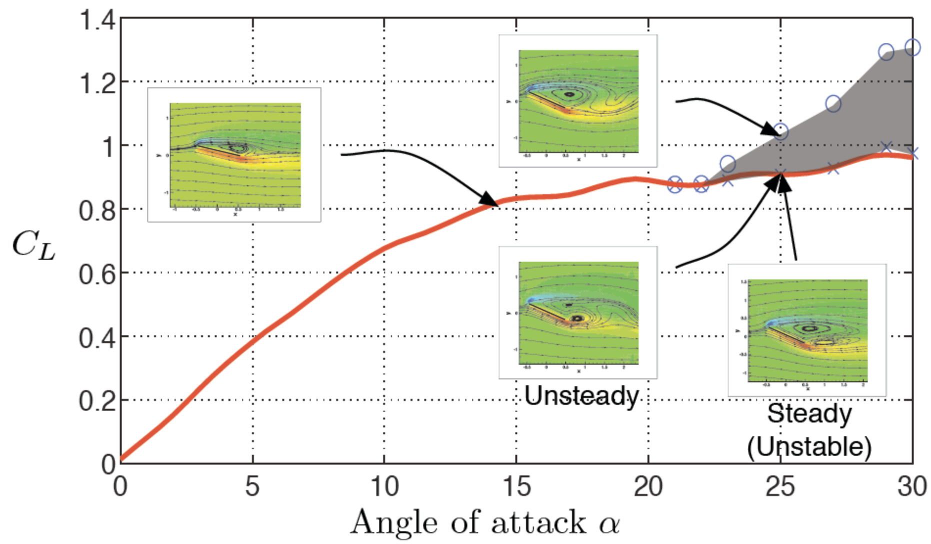

- **Are there high-lift unstable steady states in low aspect ratio airfoils?**

Model problem

Re **= 100**

AoA = 25 or 35

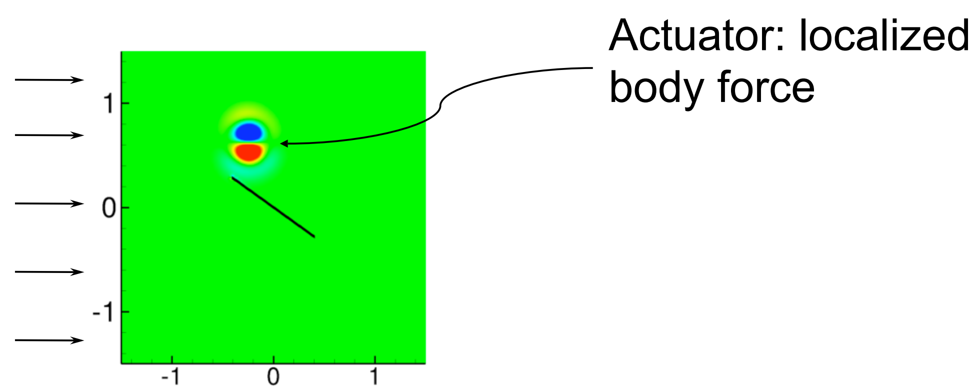

- A fast null-space based immersed boundary scheme for numerical simulations (T. Colonius and K. Taira, CMAME, 2007)

Steady state analysis

- Compute steady states using a wrapper around the DNS

DNS

$$u^k \longrightarrow \boxed{\Phi_T(u^k;\mu)} \longrightarrow u^{k+T}$$

$$\text{Define: } g(u) = u^T - u$$

- Solve for zeroes of *g(u)* using Newton-GMRES

Barkley and Tuckerman,'99, Kelley, Kevrekidis, and Qiao,'02, Ahuja et al., '07

Unstable steady state, AoA = 35

- Steady state lift close to the min. lift of the unsteady case
- No leading edge vortex
- Trailing edge vortex causes reduced lift

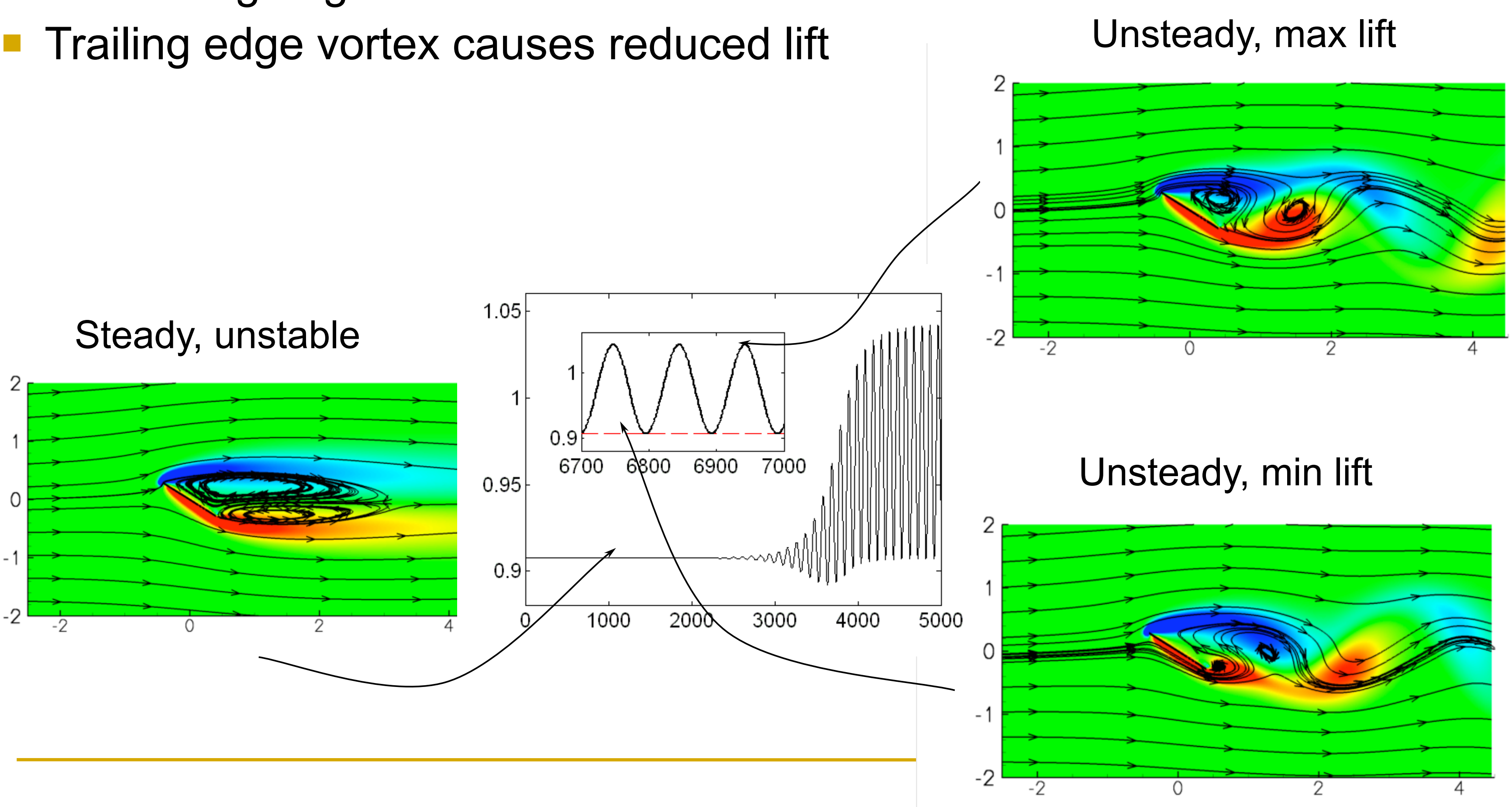

Linear stability analysis

- Find the basis spanning the unstable eigenspace of the linearized and adjoint flows
- Run the linear simulations with a zero initial condition + 10^{-8} random noise

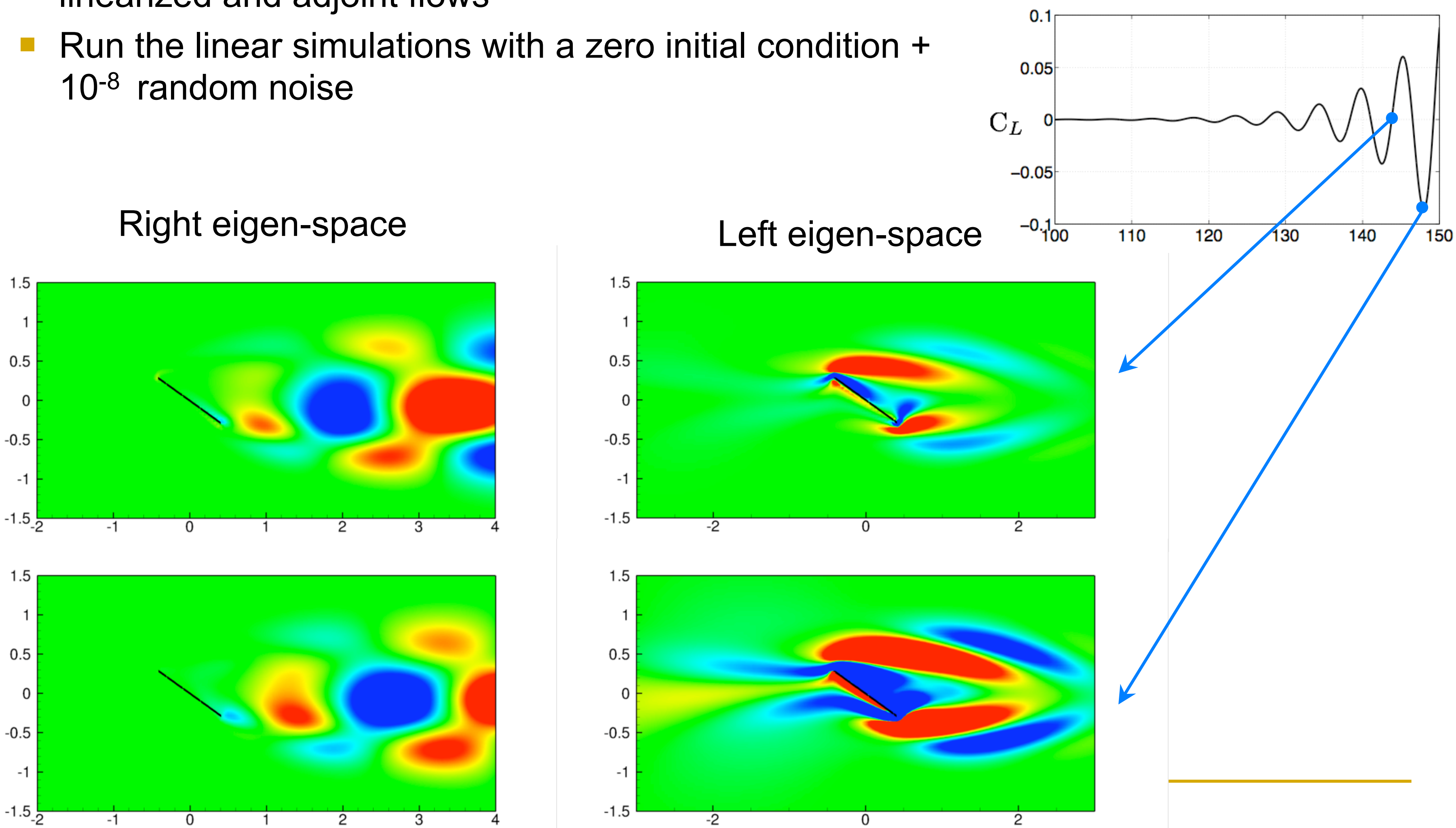

Reduced-order models for unstable systems

- Decouple stable and unstable subspaces
- Obtain balancing transformation for the stable subspace

$$\frac{d}{dt}\begin{pmatrix} x_s \\ x_u \end{pmatrix} = \begin{pmatrix} A_s & 0 \\ 0 & A_u \end{pmatrix}\begin{pmatrix} x_s \\ x_u \end{pmatrix} + \begin{pmatrix} B_s \\ B_u \end{pmatrix} u$$

- Snapshot based procedure: project out the unstable component at each time step

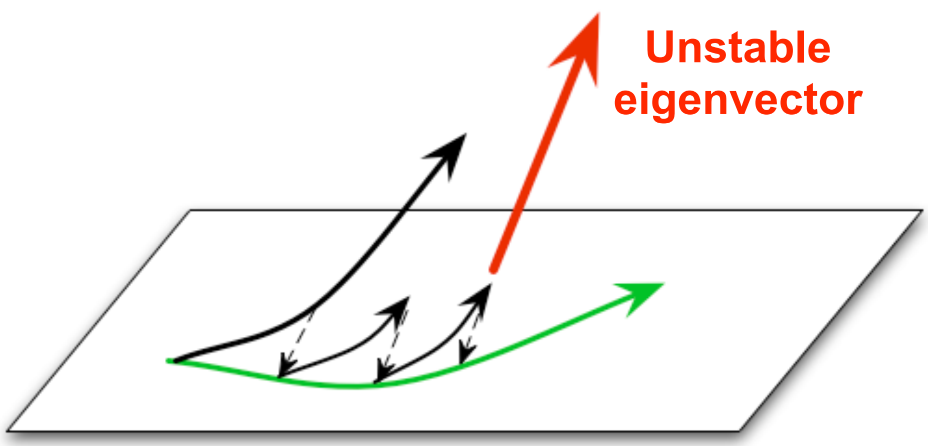

Balanced truncation for unstable systems, Zhou et al., '99

Model reduction: unstable system

Linearized NS eqns, 10^5

$$u \longrightarrow \boxed{\frac{d}{dt}\begin{pmatrix}x_s\\ x_u\end{pmatrix} = \begin{pmatrix}A_s & 0\\ 0 & A_u\end{pmatrix}\begin{pmatrix}x_s\\ x_u\end{pmatrix} + \begin{pmatrix}B_s\\ B_u\end{pmatrix}u} \longrightarrow \boxed{y = \begin{pmatrix}\Theta^T x_s\\ x_u\end{pmatrix}} \longrightarrow$$

y_s = proj. of x_s onto POD modes

x_u = unstable state

$$\mathrm{x}_s = \Phi a_s$$

$$\Psi^T \Phi = I$$

Reduced order model, 10-50 eqns.

$$u \longrightarrow \boxed{\frac{d}{dt}\begin{pmatrix}a_s\\ x_u\end{pmatrix} = \begin{pmatrix}\Psi^T A_s \Phi & 0\\ 0 & A_u\end{pmatrix}\begin{pmatrix}a_s\\ x_u\end{pmatrix} + \begin{pmatrix}\Psi^T B_s\\ B_u\end{pmatrix}u} \longrightarrow \begin{pmatrix}y_s\\ x_u\end{pmatrix}$$

Impulse response: stable subspace

- Project out the unstable component from the initial condition

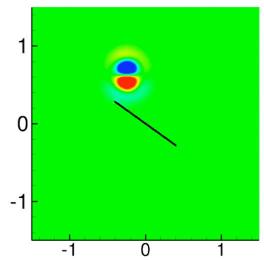

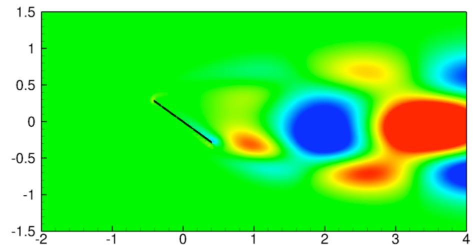

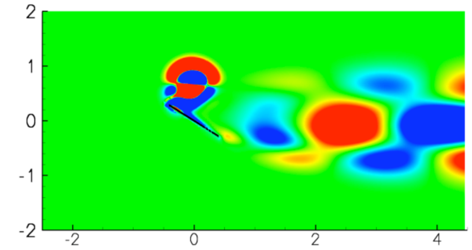

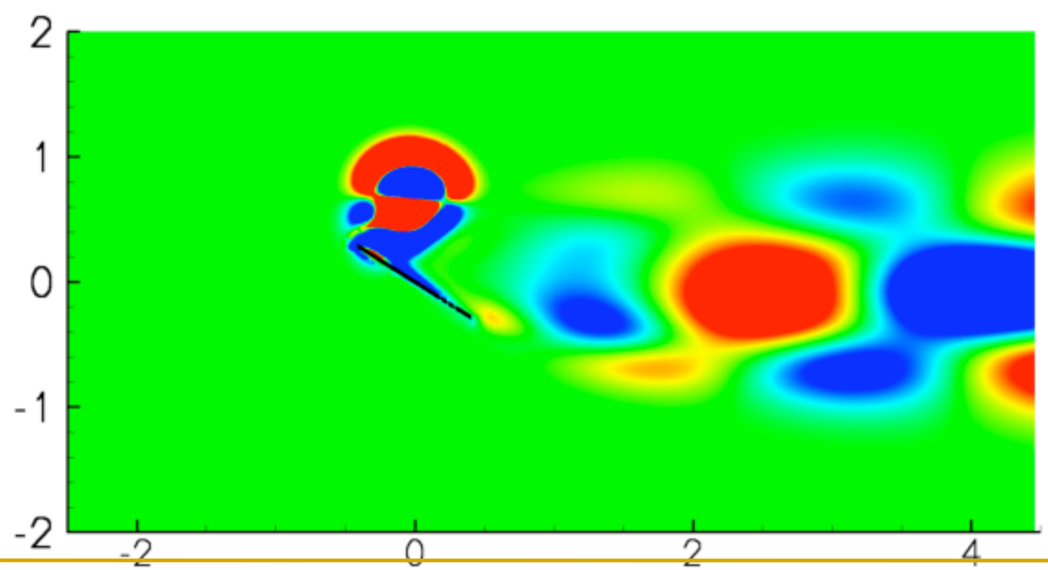

Vorticity contours:
Positive in red and
negative in blue

Adjoint impulse response

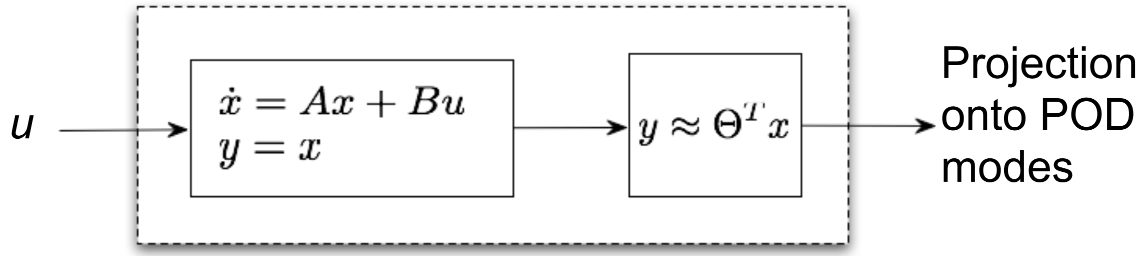

Mode 1

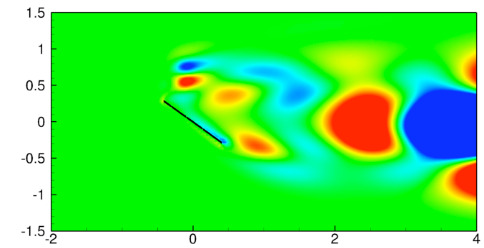

Mode 2

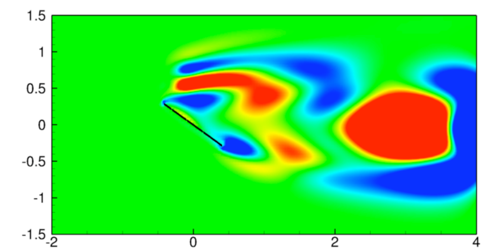

- Four POD modes capture 95% energy
- Adjoint solves with these POD modes as initial conditions

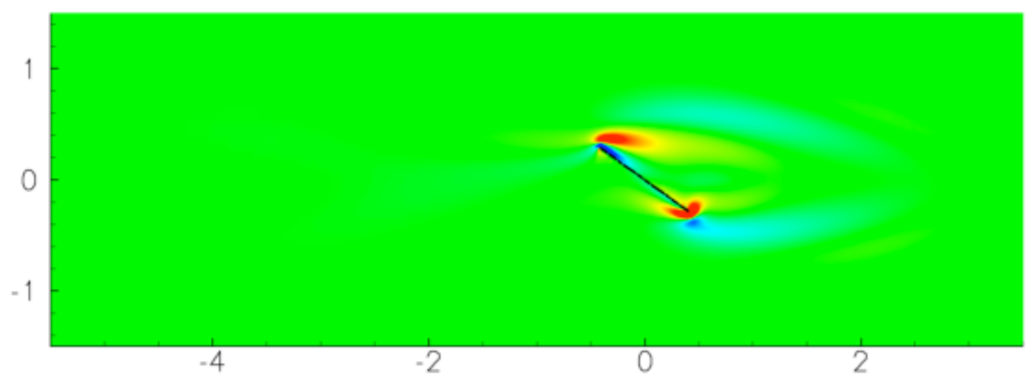

Balancing modes: stable subspace

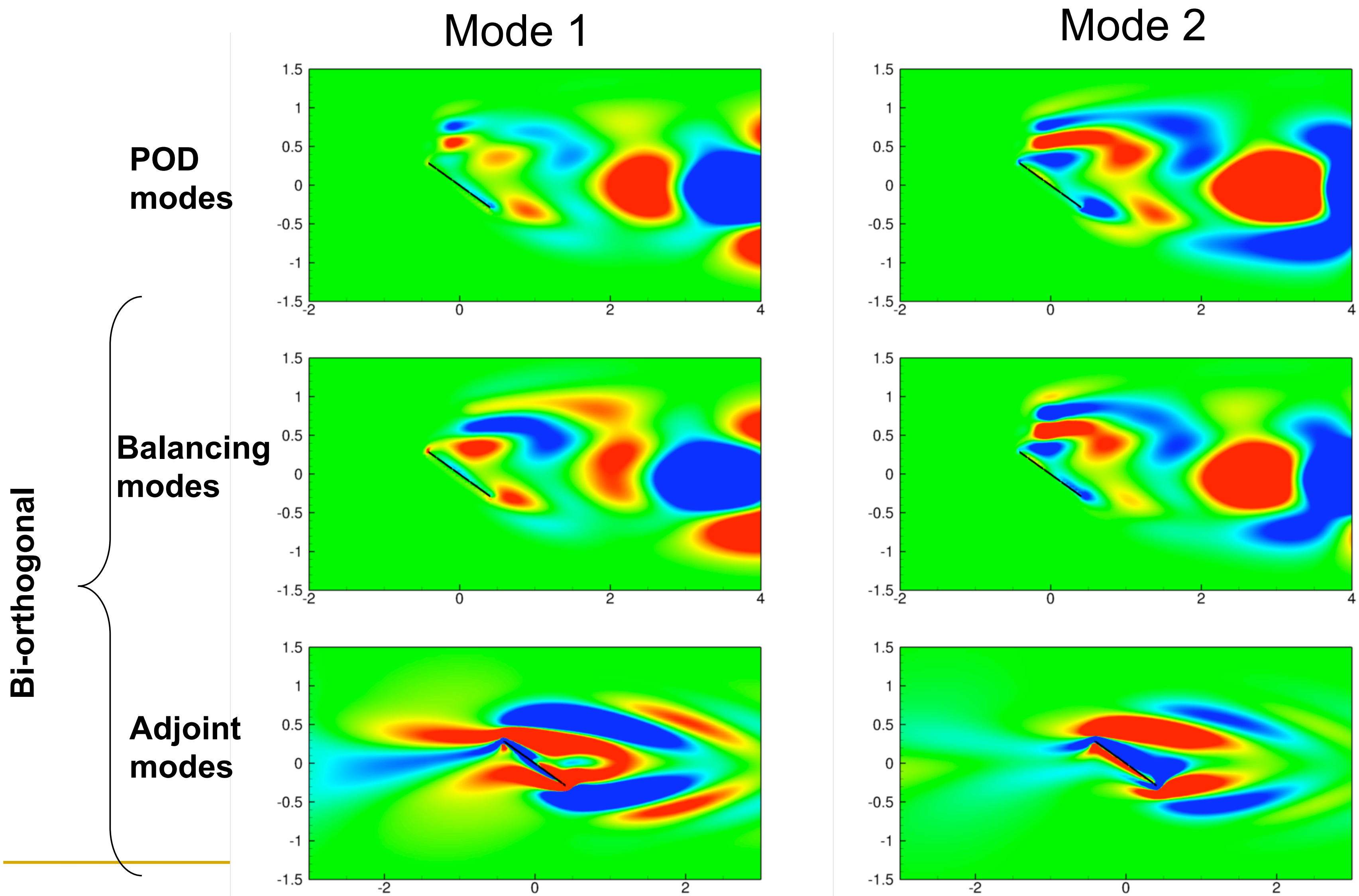

Model results: controlled case

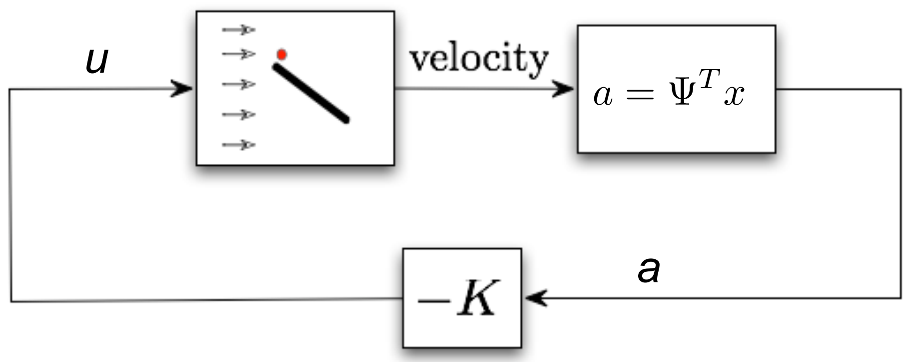

- Control based on a 10-mode model
- Gain K using LQR

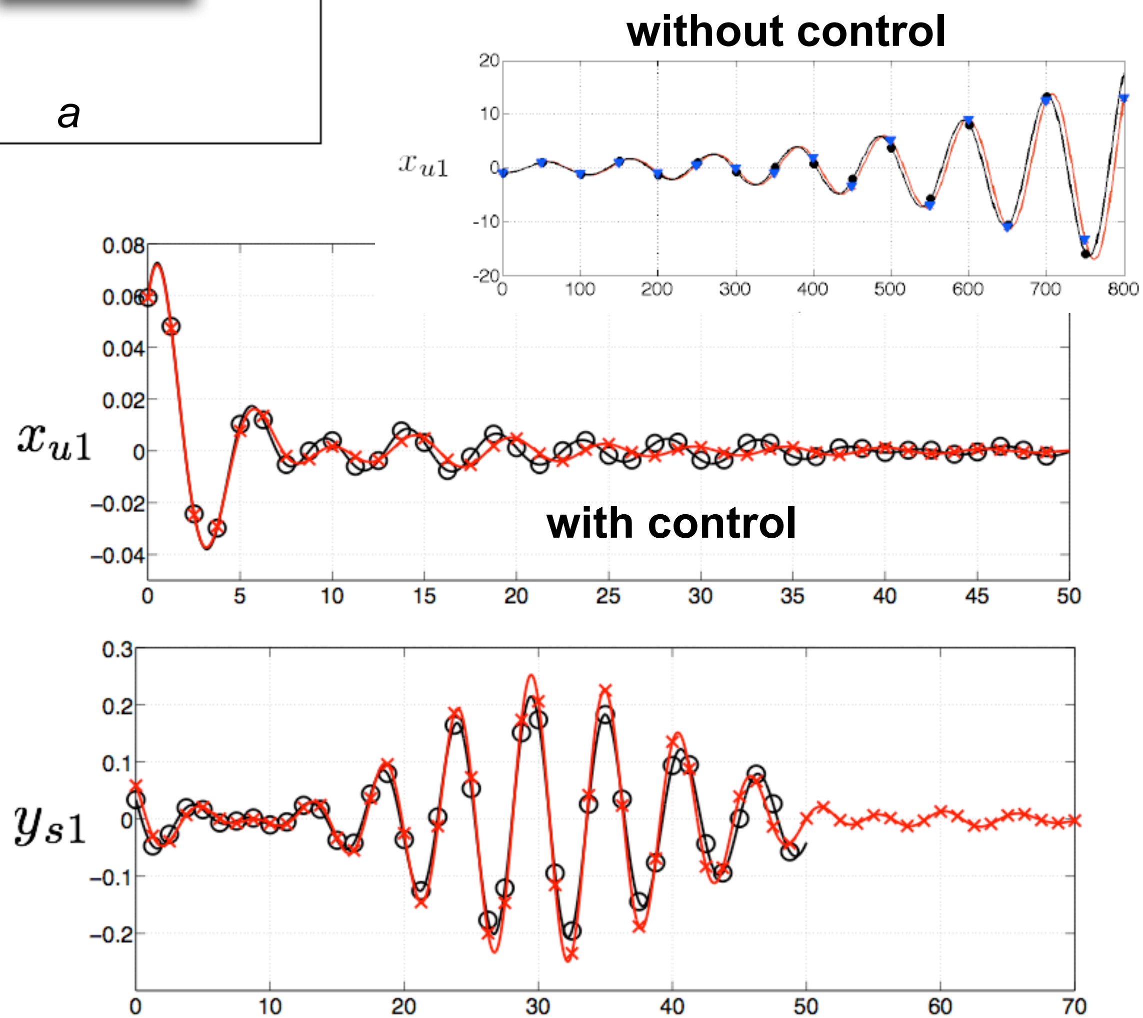

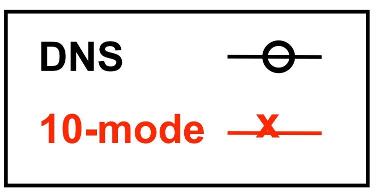

Control in full nonlinear system: close to steady state

Results of an 8-mode model

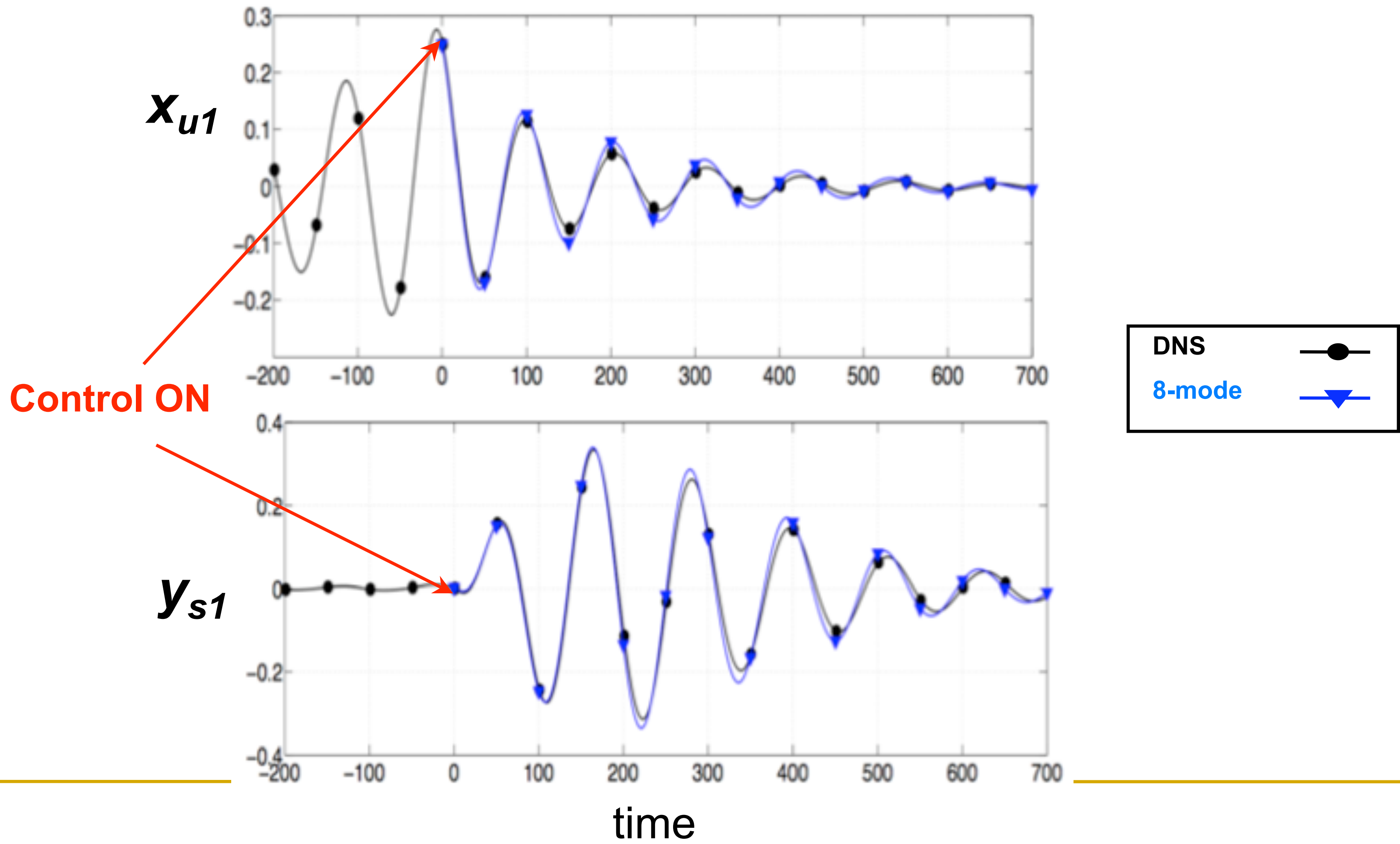

Feedback stabilization at AoA=25

- Full state feedback
- Large domain of attraction even in the full NL system
- Controller suppresses the vortex shedding

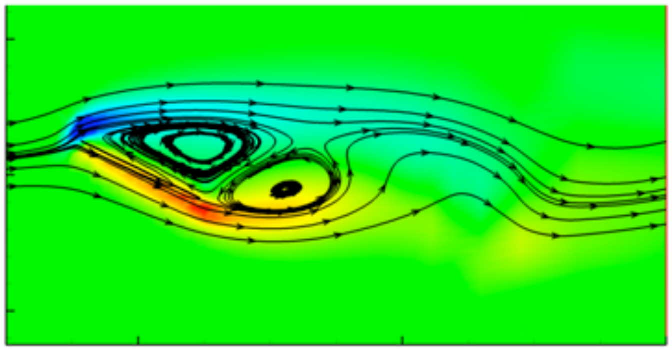

No control

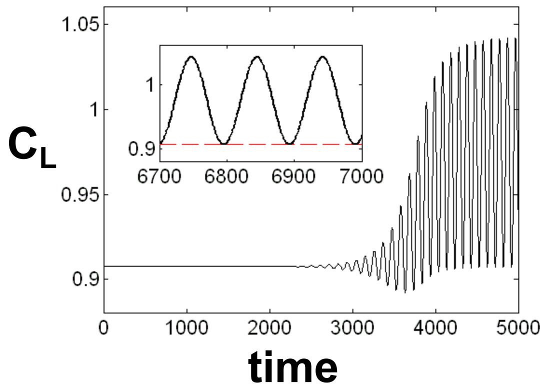

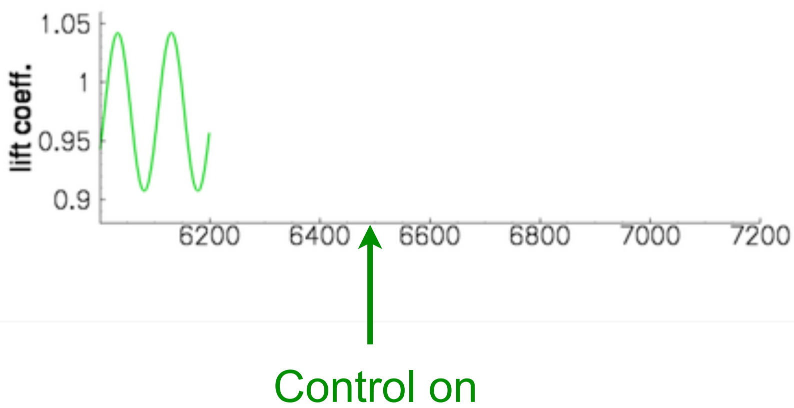

Observer design: velocity sensors

- 3 velocity sensors
- Compare projections onto 4 and 20 POD modes
- L2-norm looks similar, but the velocities at sensor locations are poorly captured by 4 POD modes

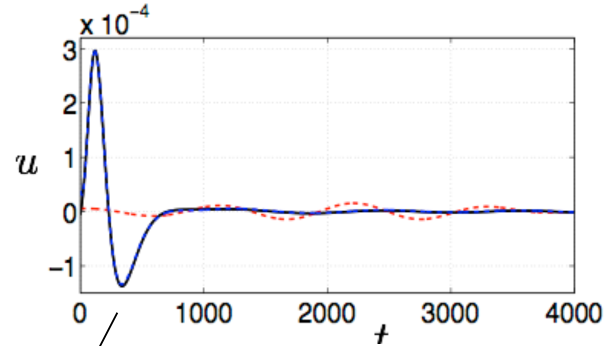

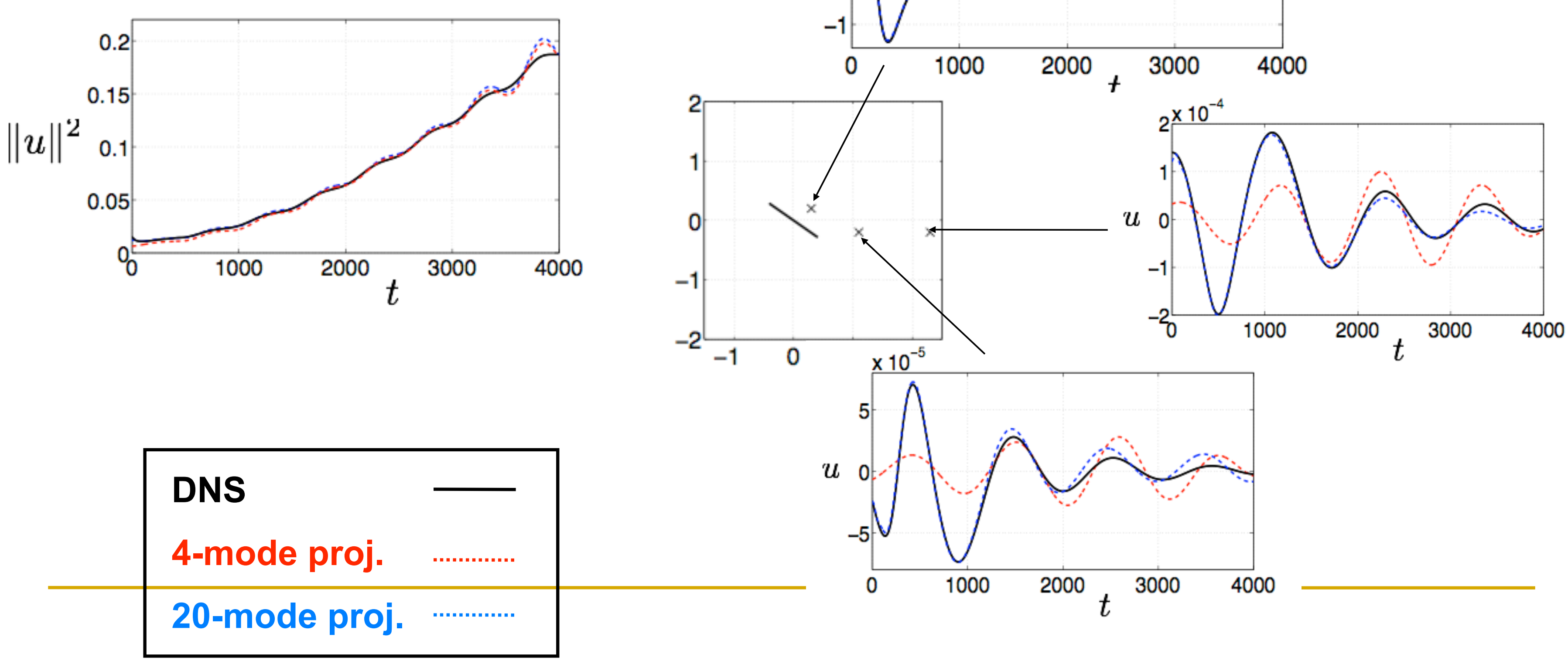

Observer based control

- Observer gain obtained using LQG
- Compensator stabilizes the steady state, but there is residual noise due to the errors in modeling the system and the measurements

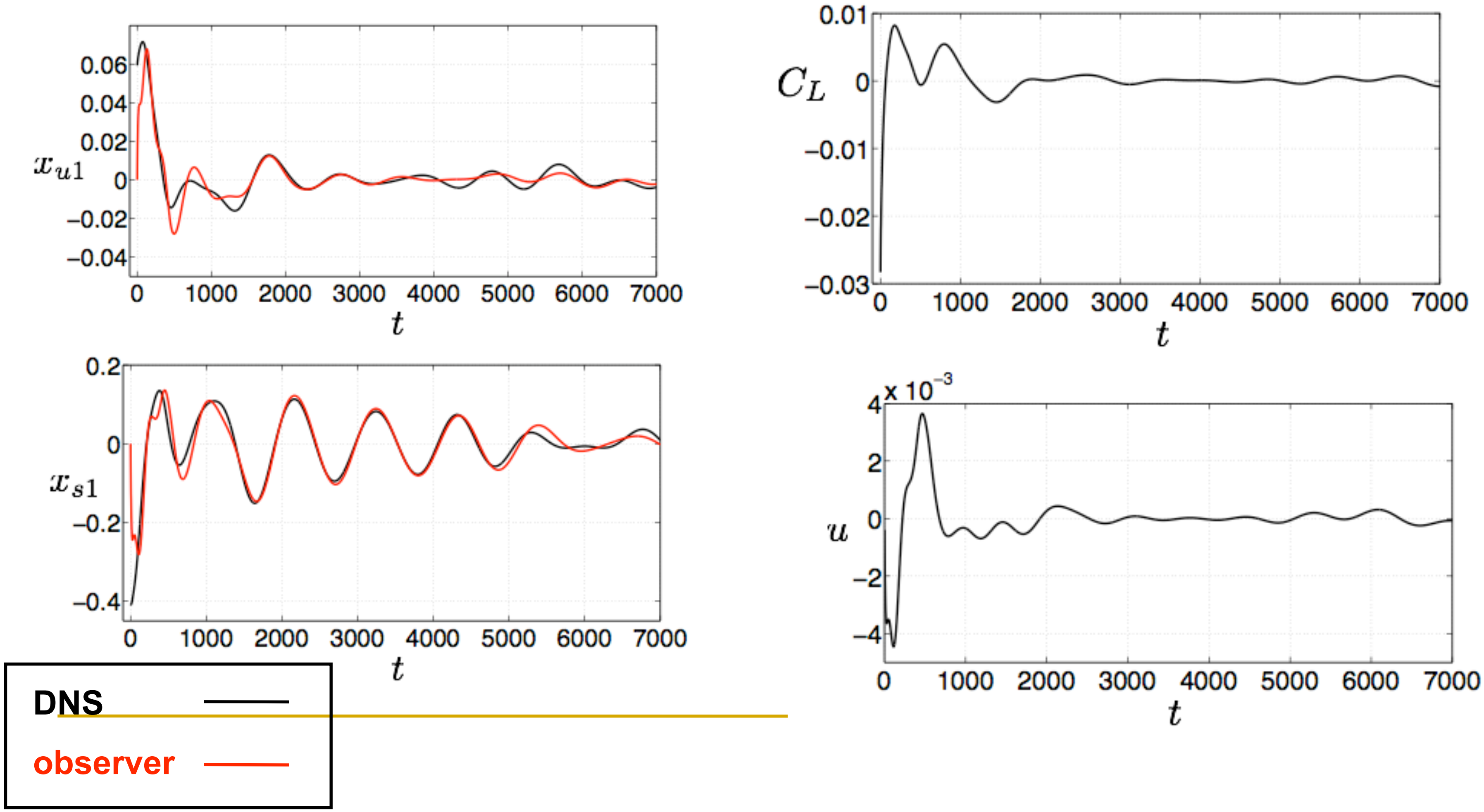

Outline

- Approximate balanced truncation using POD
  - Importance of inner product for Galerkin projection
  - Balanced truncation
  - Method of snapshots
- Applications
  - Linearized channel flow
  - Separating flow past an airfoil
- Dynamically scaling POD modes
  - Free shear layer
  - Scaled basis functions
  - Template fitting
  - Equations for the shear layer thickness

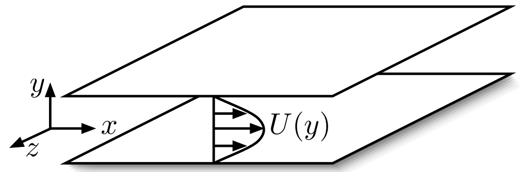

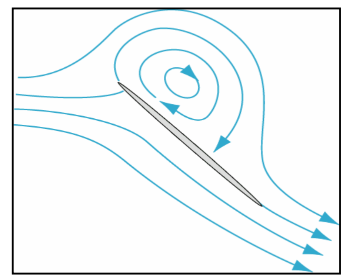

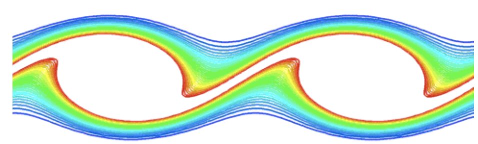

Modeling free shear layers

- Evolution history of thickness for temporal shear layer (spatially periodic):

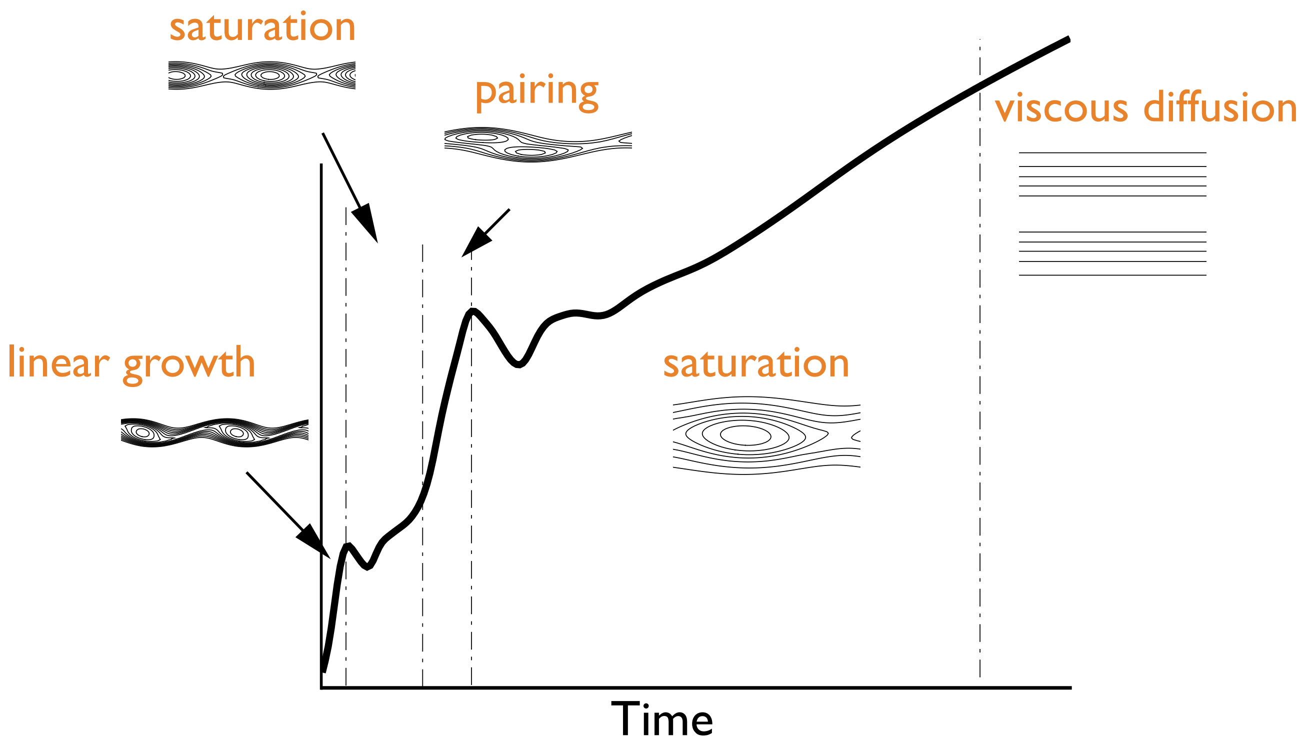

- Model initial linear growth, saturation, pairing, and eventual viscous diffusion

Methodology

- Scale POD modes dynamically in y direction to account for shear layer spreading
- Scaling invariants:
  - divergence of velocity field
  - inner product
- Key idea: template fitting
- Main result: an equation for the shear layer spreading rate:
  - as usual, also get equations for time coefficients of POD modes

Scaling basis functions

- Write solution in scaled reference frame

$$\mathbf{q} = (u, v)$$

$$\mathbf{q}(x, y, t) = G(g)\tilde{\mathbf{q}}(x, g(t)y, t)$$

- Choose $G(g) = \begin{bmatrix} 1 & 0 \\ 0 & 1/g \end{bmatrix}$: $\boxed{\text{div } \mathbf{q} = \text{div } \tilde{\mathbf{q}}}$
- Expand scaled variable $\tilde{\mathrm{q}}$ in terms of POD modes

$$\tilde{\mathbf{q}}(x, y, t) = \mathbf{u}_0(y) + \sum_{j=1}^{n} a_j(t)\varphi_j(x, y)$$

- Advantage of the scaling: capture similar-looking structures as shear layer spreads
- Advantage of divergence-invariant mapping: auto-satisfy continuity equation; simplify pressure term

Template fitting

- How do we choose the scaling g(t)?
  - Choose g(t) so that $\tilde{\mathbf{q}}(x,y,t)$ lines up best with a preselected template (here, the base flow):

$$\frac{d}{ds}\bigg|_{s=0} \|\tilde{\mathbf{q}}(x,y,t) - \mathbf{u}_0(x,h(s)y)\|^2 = 0$$

for any curve $h(s) > 0$ with $h(0) = 1$

  - This means the scaled solution $\tilde{\mathbf{q}}(x,y,t)$ satisfies

$$\left\langle y\frac{\partial \mathbf{u}_0}{\partial y}, \tilde{\mathbf{q}} - \mathbf{u}_0 \right\rangle = 0$$

  - Geometrically, the set of all "properly scaled" functions $\tilde{\mathbf{q}}$ is an affine space through $\mathbf{u}_0$ and orthogonal to $y\partial_y \mathbf{u}_0$
  - This enables one to write dynamics for how the thickness g(t) evolves

$$\frac{\dot{g}}{g} = \frac{\left\langle f_g^1(\tilde{u}), y\partial_y u_0 \right\rangle}{\langle y\partial_y \tilde{u}, y\partial_y u_0 \rangle}$$

Equation for evolution of the thickness

- How does g(t) evolve in time?
  - We have a constraint ($\tilde{\mathbf{q}}(x,y,t)$ lines up best with template $\mathbf{u}_0$):

$$\left\langle y\frac{\partial \mathbf{u}_0}{\partial y}, \tilde{\mathbf{q}} - \mathbf{u}_0 \right\rangle = 0$$

  - Differentiate:

$$\left\langle y\frac{\partial \mathbf{u}_0}{\partial y}, \frac{\partial \tilde{\mathbf{q}}}{\partial t} \right\rangle = 0$$

  - Use equations of motion

$$\frac{\partial \tilde{\mathbf{q}}}{\partial t} = f_g(\tilde{\mathbf{q}}) - \frac{\dot{g}}{g} y \frac{\partial \tilde{\mathbf{q}}}{\partial y} - G(1/g)\dot{G}(g,\dot{g})\tilde{\mathbf{q}}(x,y,t)$$

  - This gives an equation for g:

$$\boxed{\frac{\dot{g}}{g} = \frac{\langle f_g^1(\tilde{u}), y\partial_y u_0 \rangle}{\langle y\partial_y \tilde{u}, y\partial_y u_0 \rangle}}$$

Galerkin equations for the shear layer

- Equation for the POD mode coefficients:
  - retain only modes k=1, n=1 and 2:

$$\dot{a}_{1,1} = \frac{g^2 c_{11g} + c_{11}}{g^2 n_{1g} + n_1} a_{1,1} + \frac{g^2 c_{12g} + c_{12}}{g^2 n_{1g} + n_1} a_{1,2} + \frac{1}{\mathrm{Re}} \left[-(\frac{2\pi}{L})^2 + \frac{g^2 d_{1g} + d_1}{g^2 n_{1g} + n_1} g^2 \right] a_{1,1} + \frac{g^2 e_{1g} + e_1}{g^2 n_{1g} + n_1} \frac{\dot{g}}{g} a_{1,1},$$

$$\dot{a}_{1,2} = \frac{g^2 c_{21g} + c_{21}}{g^2 n_{2g} + n_2} a_{1,1} + \frac{g^2 c_{22g} + c_{22}}{g^2 n_{2g} + n_2} a_{1,2} + \frac{1}{\mathrm{Re}} \left[-(\frac{2\pi}{L})^2 + \frac{g^2 d_{2g} + d_2}{g^2 n_{2g} + n_2} g^2 \right] a_{1,2} + \frac{g^2 e_{2g} + e_2}{g^2 n_{2g} + n_2} \frac{\dot{g}}{g} a_{1,2},$$

- Equation for the scaling g:

$$\dot{g} = \frac{c_{01}}{n_0} a_{1,1} a_{1,1}^* g + \frac{c_{02}}{n_0} a_{1,2} a_{1,2}^* g + \frac{c_{03}}{n_0} a_{1,1} a_{1,2}^* g + \frac{c_{04}}{n_0} a_{1,2} a_{1,1}^* g + \frac{1}{\mathrm{Re}} \frac{d_0}{n_0} g^3$$

- Retaining modes k=1 and 2, n=1 and 2 also tractable, but messy

- Use inner product that is preserved under scaling:

$$\langle \tilde{\mathbf{q}}_1, \tilde{\mathbf{q}}_2 \rangle_g = \int_\Omega (\frac{1}{g} \tilde{u}_1 \tilde{u}_2 + \frac{1}{g^3} \tilde{v}_1 \tilde{v}_2) dx dy$$

Results

- Base flow with small perturbation
  - Base flow: $u_0 = U_c \mathrm{erfc}(\eta), \quad \eta = \frac{-y}{2g}\sqrt{\frac{\mathrm{Re}}{t_0}}$
  - Perturbation is along the unstable eigenfunction of the linearized problem
- Consider three separate cases
  - No perturbation: viscous growth
  - Initial perturbation with k=1: vortex roll-up
  - Initial perturbation with k=2:
    - vortex roll-up
    - pairing
    - k=1 mode arises through pairing

Model results: k=0

- Only one equation left for g:

$$\dot{g} = \frac{1}{\mathrm{Re}}\frac{d_0}{n_0}g^3 \quad \Longrightarrow \quad \dot{g} = -\frac{g^3}{2t_0} \quad \Longrightarrow \quad g(t) = \sqrt{\frac{t_0}{t}}$$

- Recovers exact theoretical growth rate for Stokes problem:

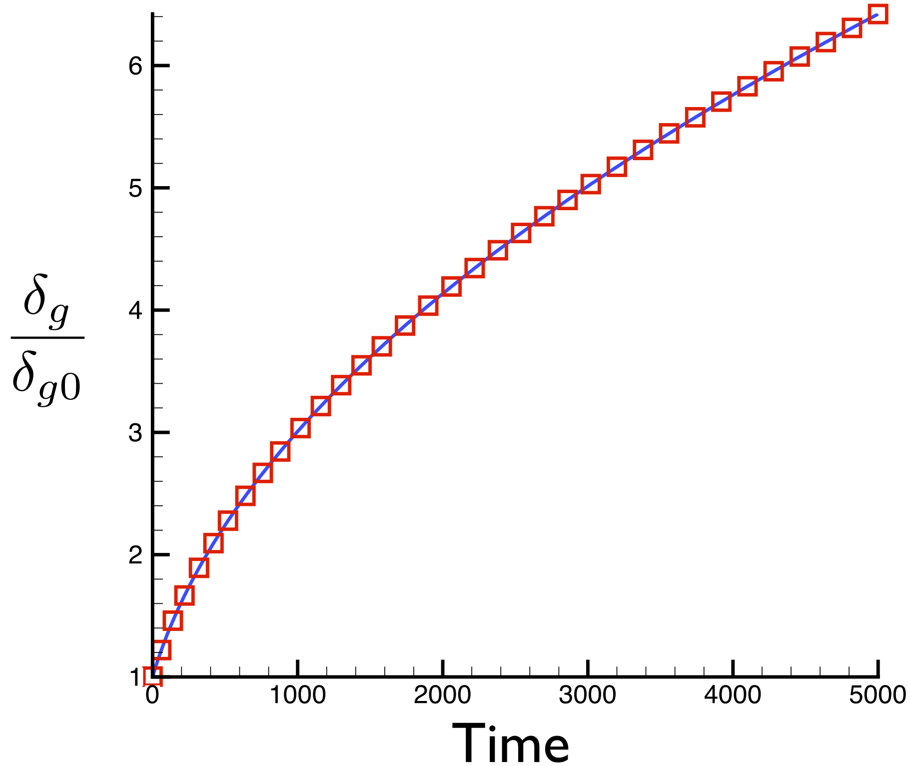

Movie of DNS

- Initial condition with k=1 (Re = 200)

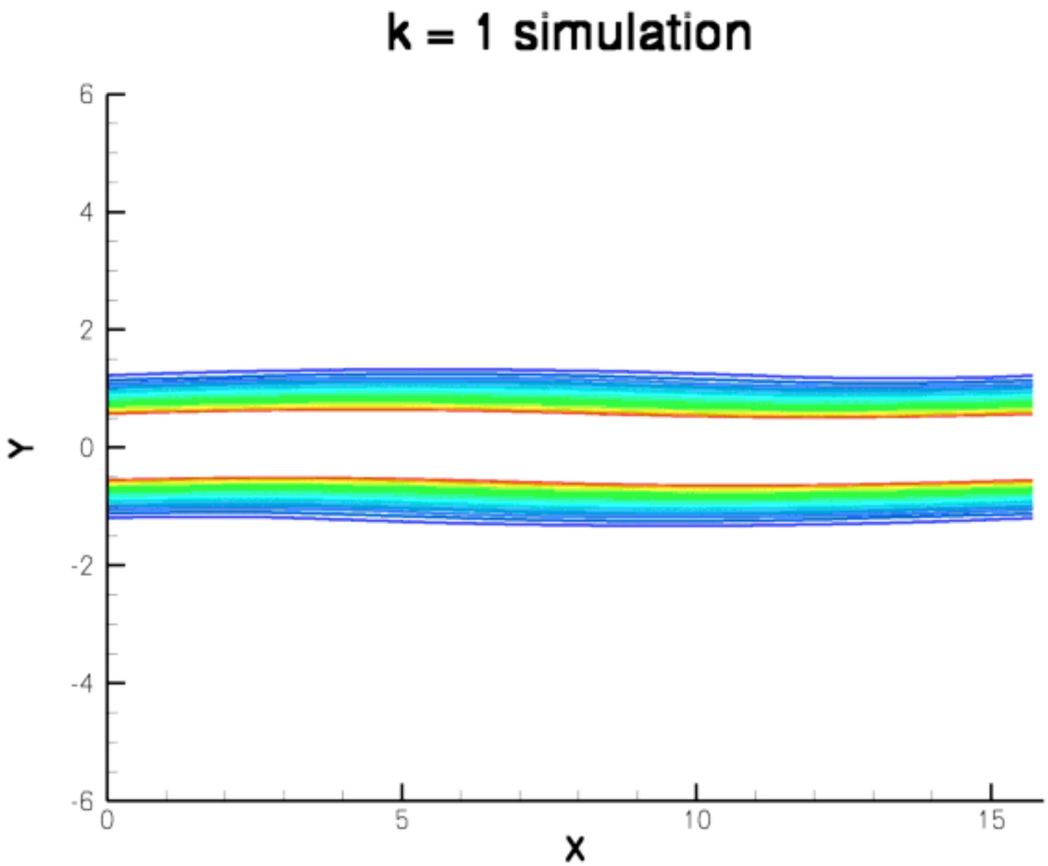

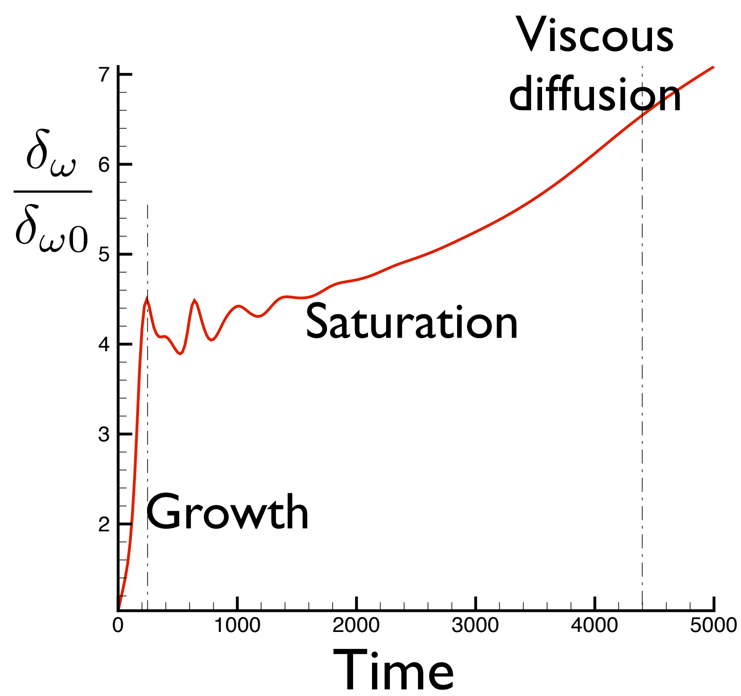

Movie of DNS

- Initial condition with k=2 (Re = 200)

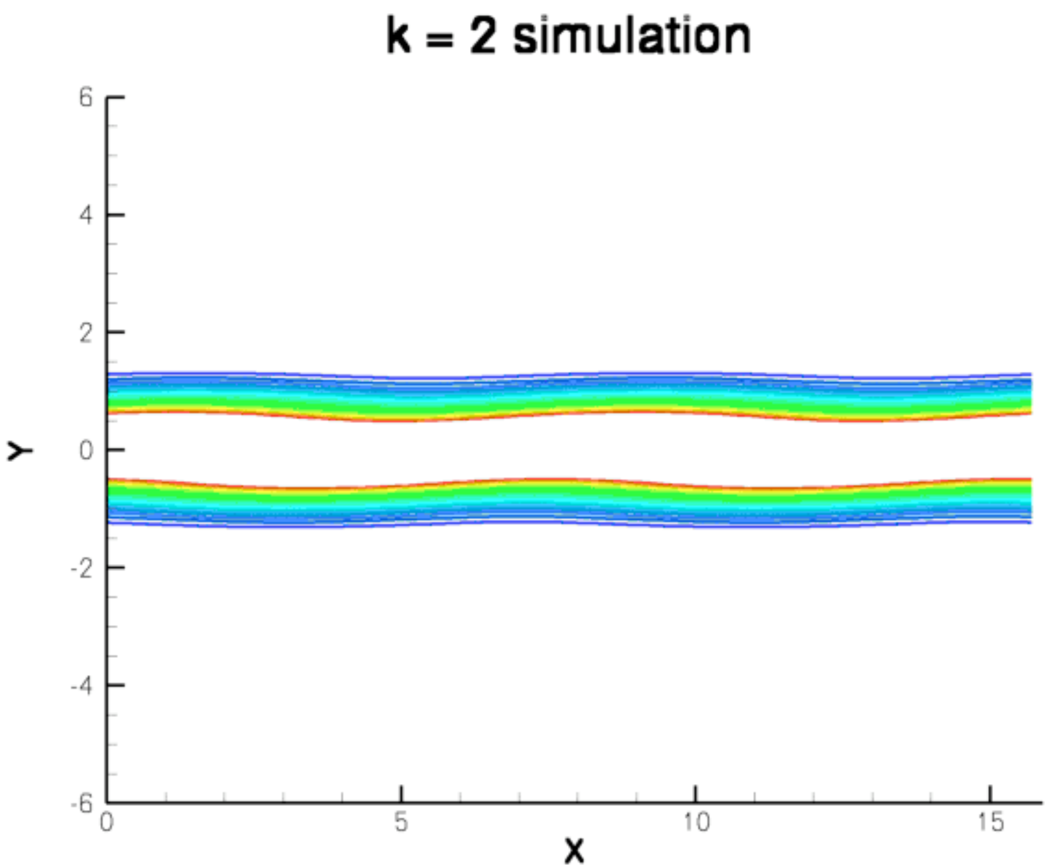

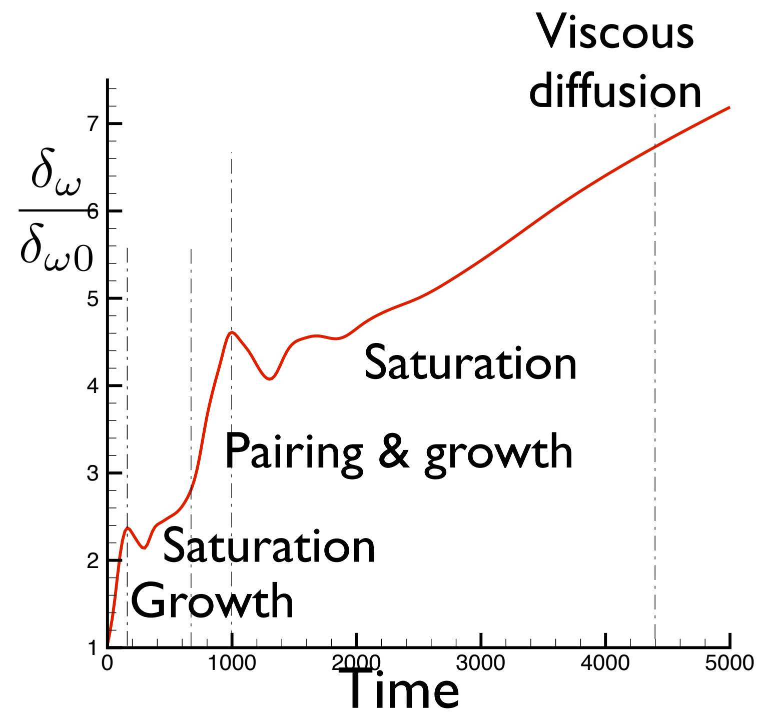

POD modes

- Energy contained in modes (k=1 initial condition)

(k,n)	lambda	Energy (%)
(1,1)	130.3	91.0
(1, 2)	6.8	4.8
(2, 1)	4.5	3.1
all k=0		0.4

  - Zero mode contains very little energy - scaling was effective at removing the mean spreading

POD modes

- Initial condition with k=1

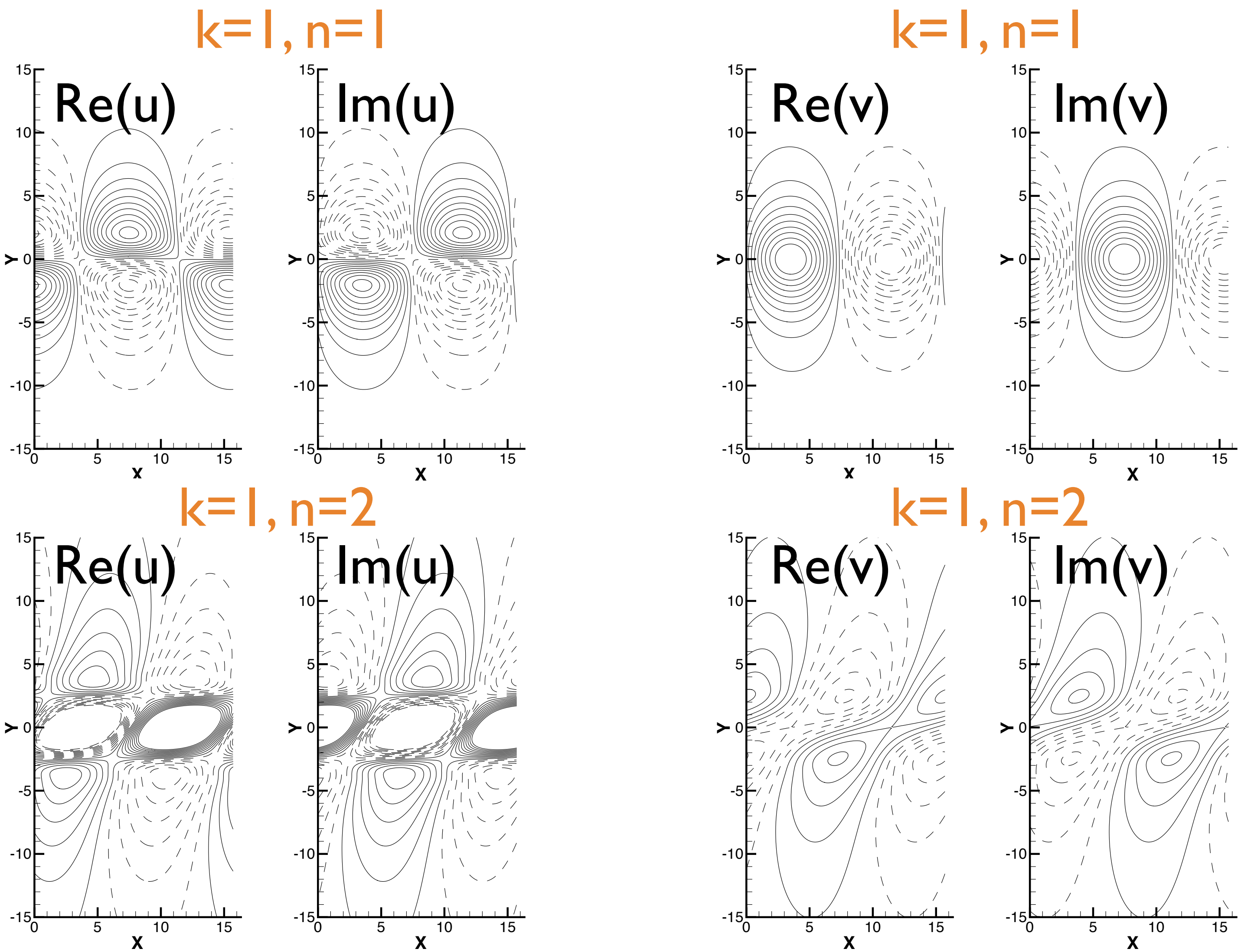

POD modes

- Energy contained in modes (k=2 initial condition)

(k,n)	lambda	Energy (%)
(1,1)	27.5	40.1
(2,1)	37.9	55.2
(1,2)	0.9	1.3
(2,2)	1.6	2.3
all k=0		0.6

  - Scaling still effective at removing the mean spreading (zero mode has small energy)

POD modes

- Initial condition with k=2

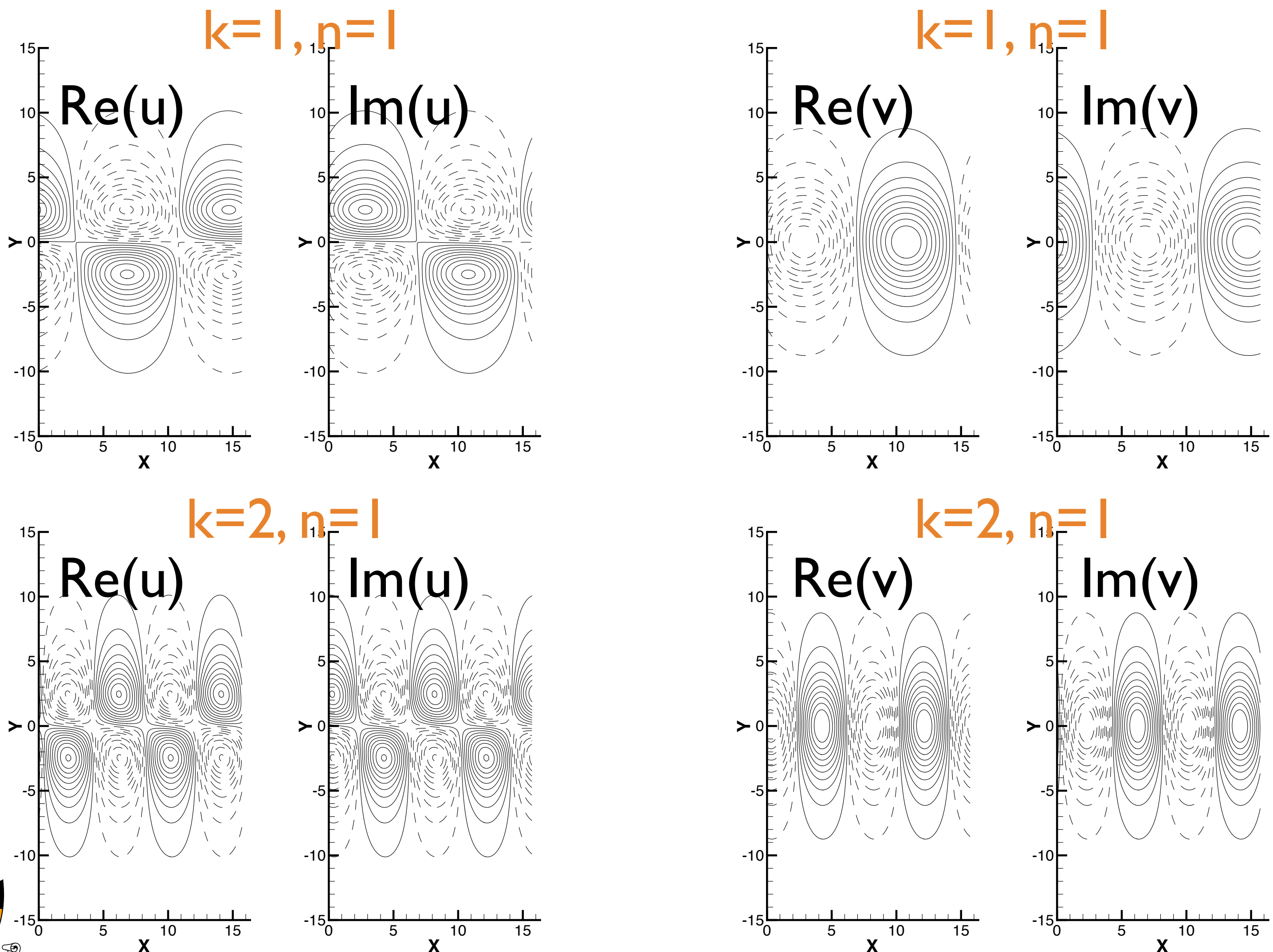

POD modes

- Initial condition with k=2

k=1, n=2

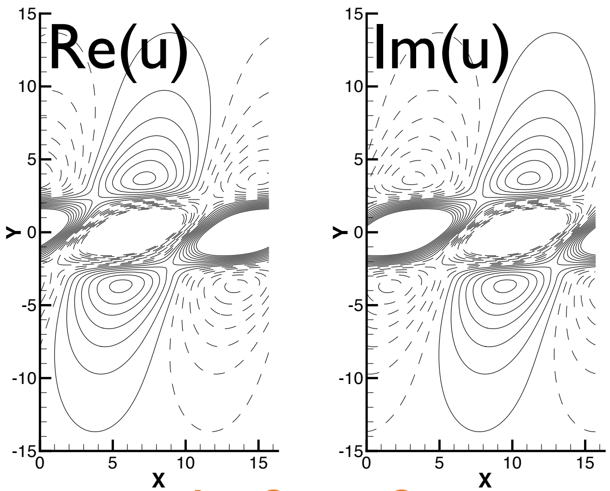

k=1, n=2

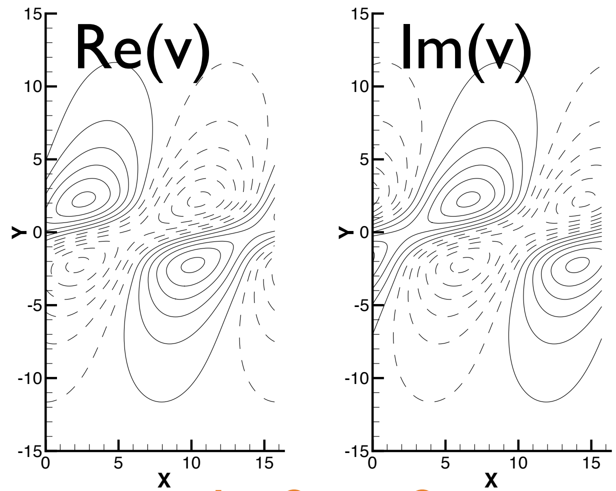

k=2, n=2

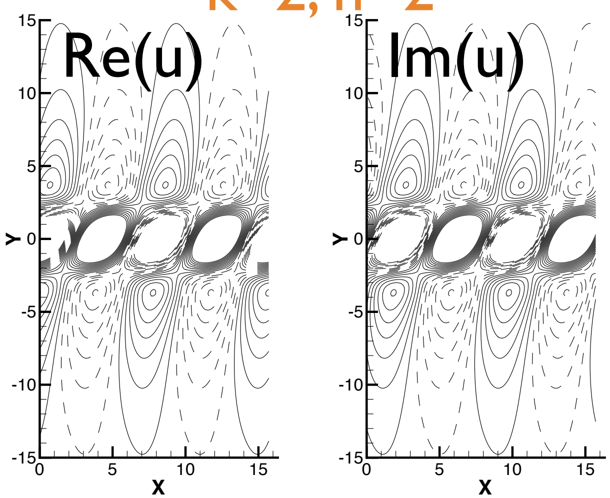

k=2, n=2

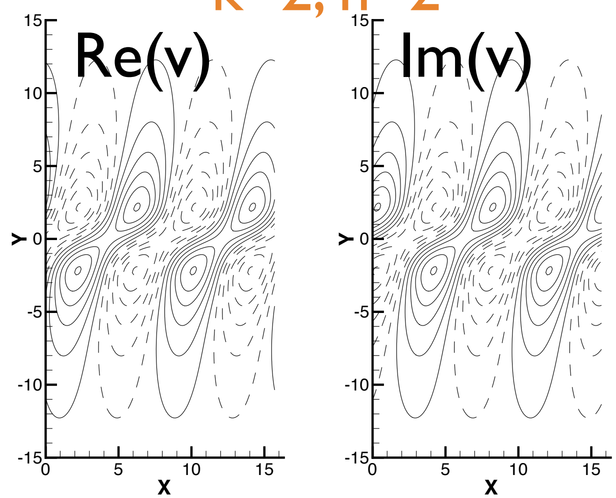

DNS v.s. Model

- Comparison of simulation and model results

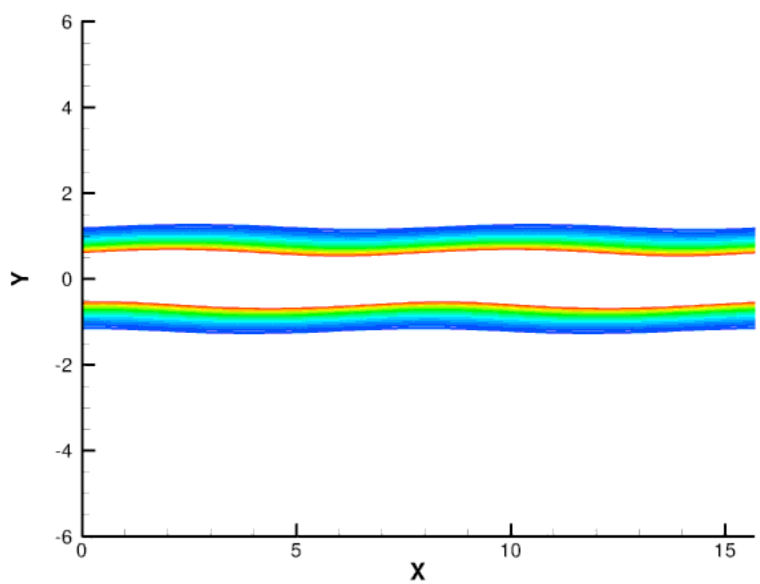

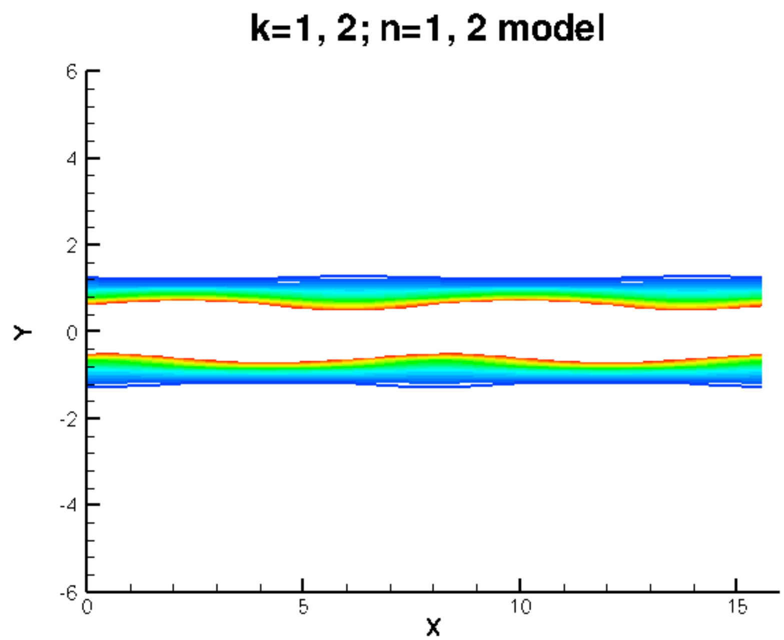

Model results: k=1

- Thickness and amplitude of POD modes for k=1 initial condition: projection of full simulation

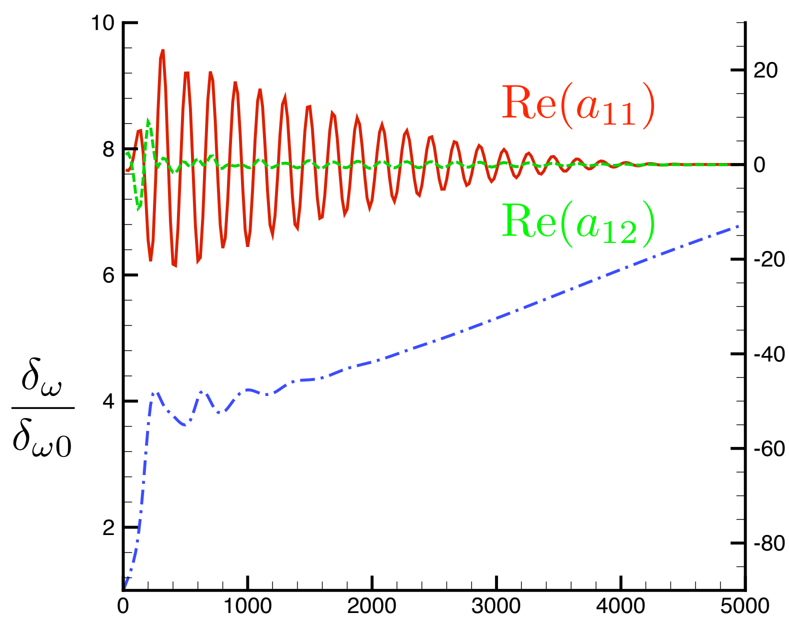

- Thickness and amplitude of POD modes for k=1 initial condition: low-dimensional model

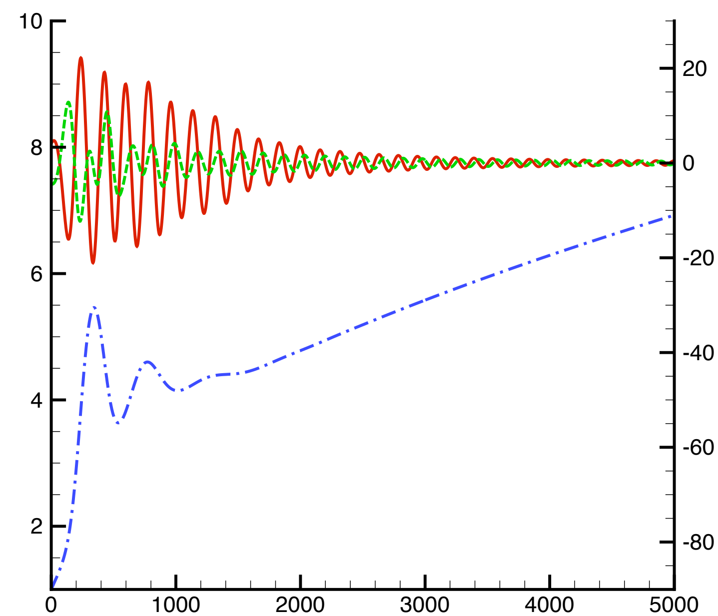

Phase shift phenomenon: Modes 1 and 2 are out of phase during linear growth, in phase after saturation

Model results: k=1

- Phase delay between the first 2 POD modes: projection of full simulation
- Phase delay between the first 2 Pod modes: low-dimensional model

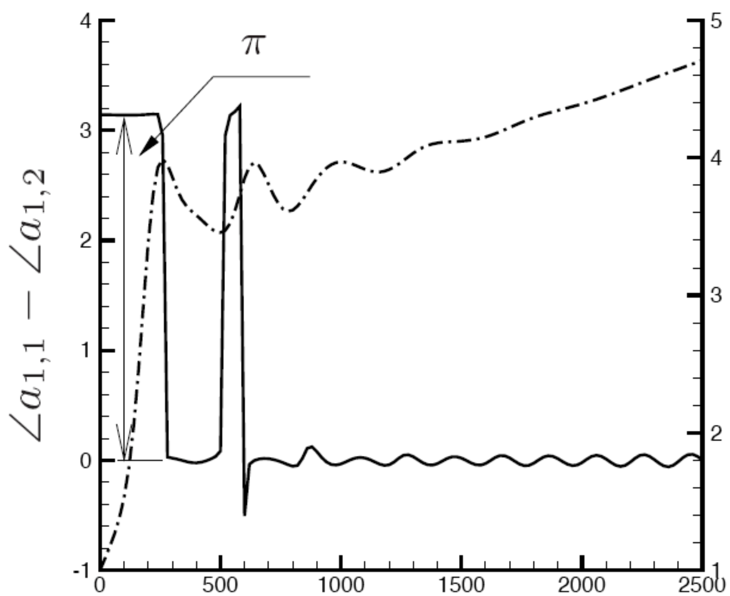

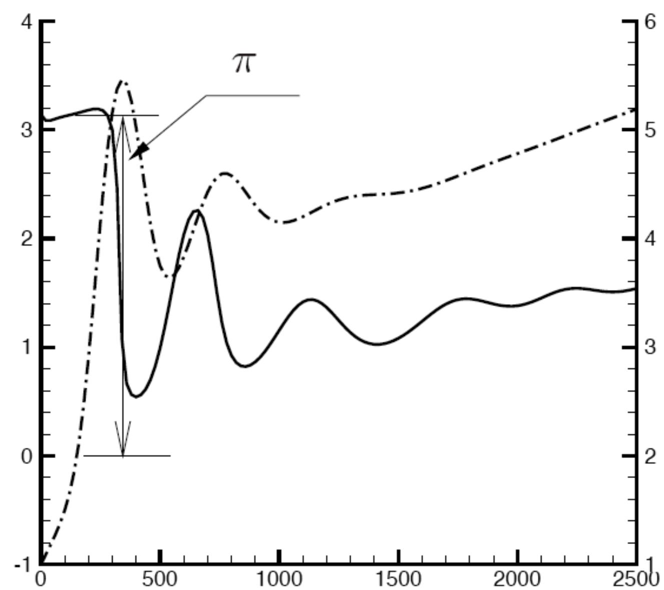

Model results: k=2

- Thickness and amplitude of POD modes for k=2 initial condition: projection of full simulation

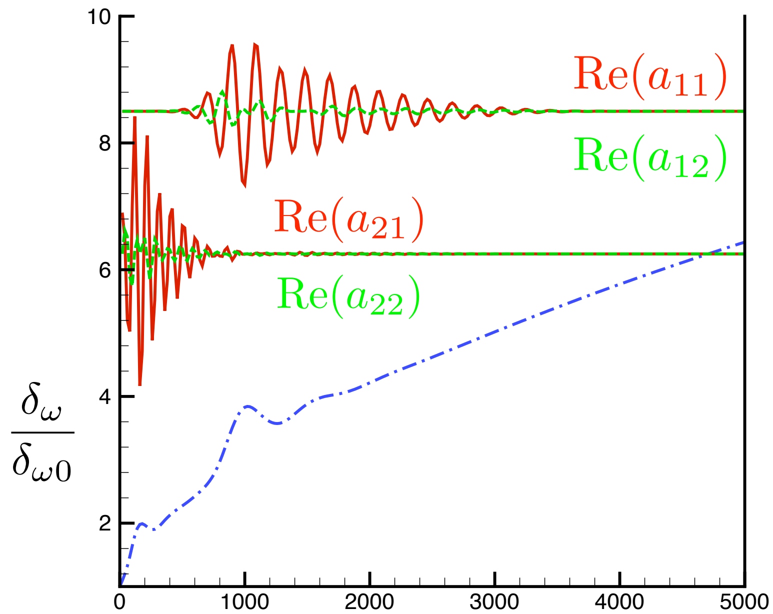

- Thickness and amplitude of POD modes for k=2 initial condition: low-dimensional model

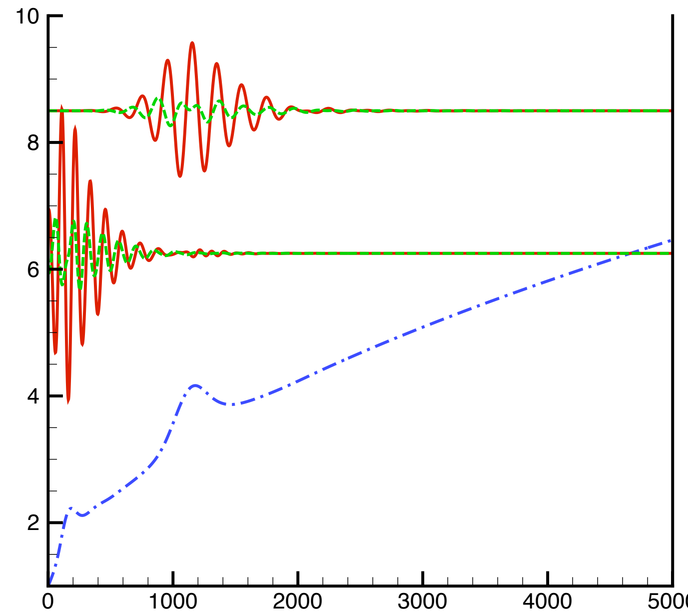

Model results: k=2

- Phase delay between the first 2 POD modes: projection of full simulation
- Phase delay between the first 2 Pod modes: low-dimensional model

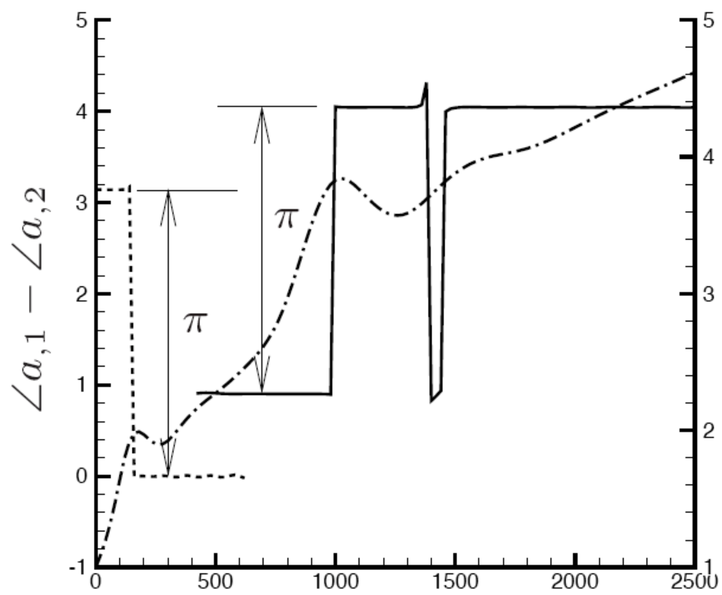

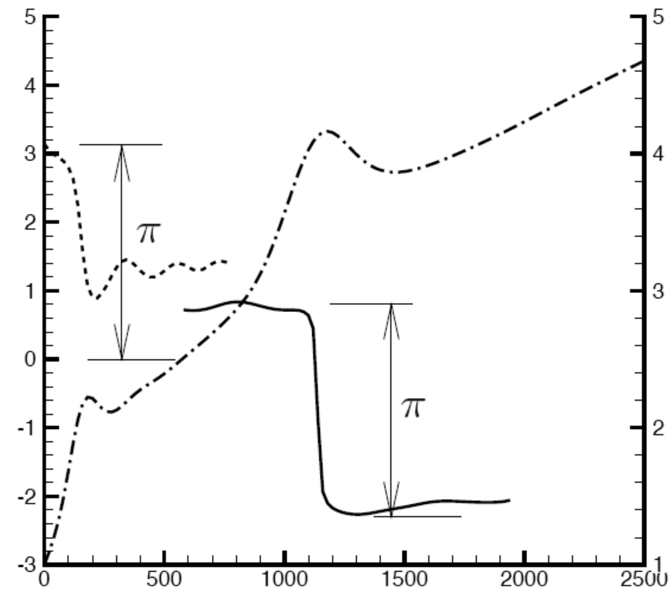

Summary

- Approximate balanced truncation
  - Approximates exact balanced truncation to as high accuracy as desired, using snapshots from linearized and adjoint simulations
  - Computational cost similar to POD, once snapshots computed
  - For a given number of modes, transients and frequency response much more accurately captured than POD models of same order
  - Extension of basic approach to model unstable linear systems
  - Feedback controllers designed from these models perform well, even on full-order, nonlinear systems
  - Extensions to (weakly) nonlinear systems straightforward
- Dynamically scaled POD modes
  - For systems with self-similar behavior, dynamic scaling decreases number of modes required
  - Temporal shear layer dynamics modeled with 4 complex modes, including linear growth, saturation, pairing, and viscous diffusion

Outlook

- Outstanding challenges
  - Combining ideas from balanced truncation with results from experimental data, where adjoints are not available
  - Systematic approach for highly nonlinear systems (far from equilibrium)
  - Reduced-order models for messy, turbulent flows. Low-dimensional models are, strictly speaking, not possible, but one is not interested in all of the details
  - New control synthesis tools needed for these classes of nonlinear systems?